中尺度氣象學

(Mesoscale Meteorology)

授課老師: 游政谷

Mesoscale(5): Severe Storms

The classification of storm types

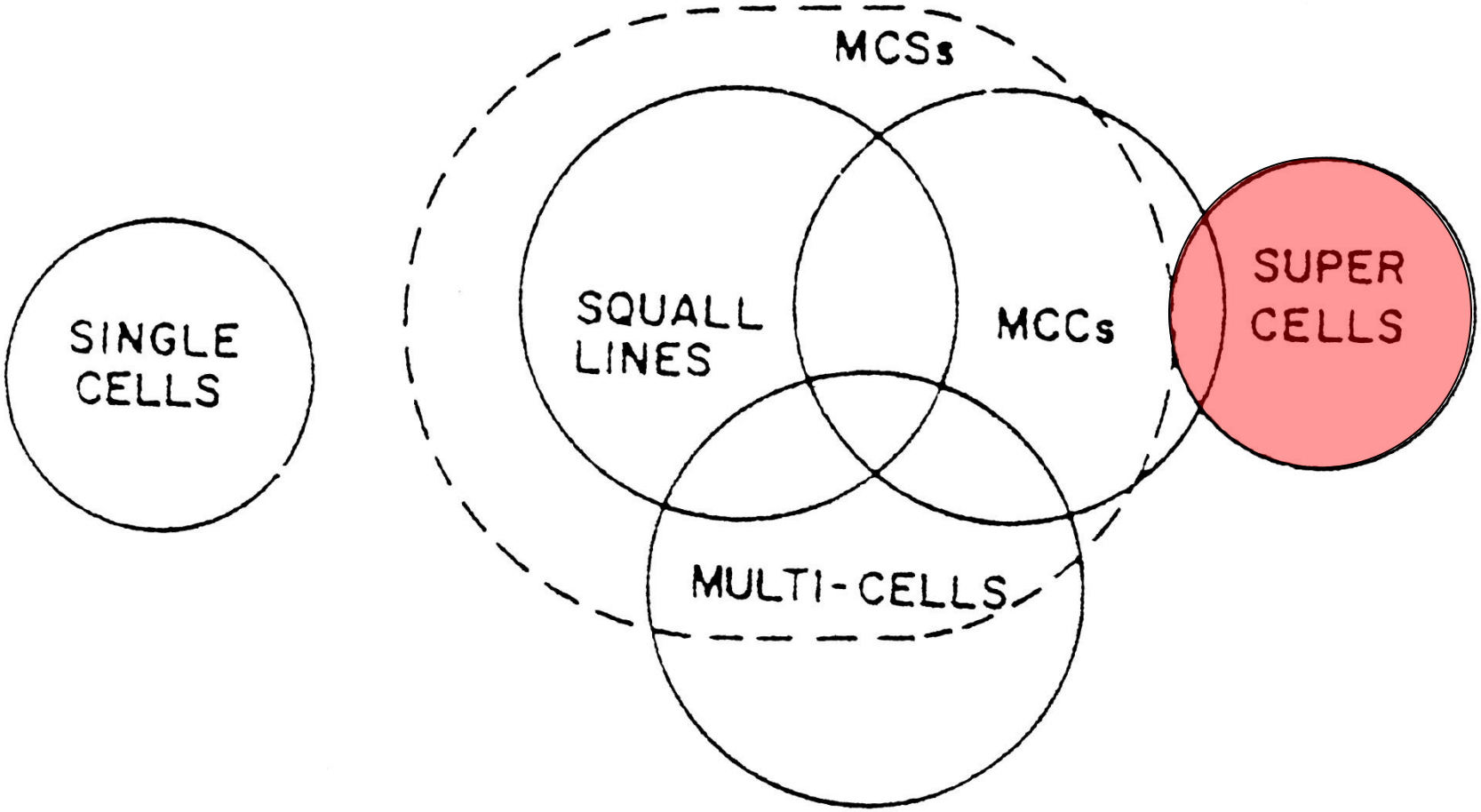

中尺度對流複合體 (Mesoscale Convective Complex)的定義 (Maddox 1980)

TABLE 9.1. Definition of mesoscale convective complex.

Size:	A—Cloud shield with continuously low infrared (IR) temperature $\leq -33°C$; must have an area $\geq 10^5$ km^2
	B—Interior cold cloud region with temperature $\leq -52°$; must have an area $\geq 0.5 \times 10^5$ km^2
Initiate:	Size definitions A and B are first satisfied
Duration:	Size definitions A and B must be met for a period ≥ 6 h
Maximum extent:	Contiguous cold cloud shield (IR temperature $\leq -33°$) reaches maximum size
Shape:	Eccentricity (minor axis/major axis) ≥ 0.7 at time of maximum extent
Terminate:	Size definitions A and B no longer satisfied

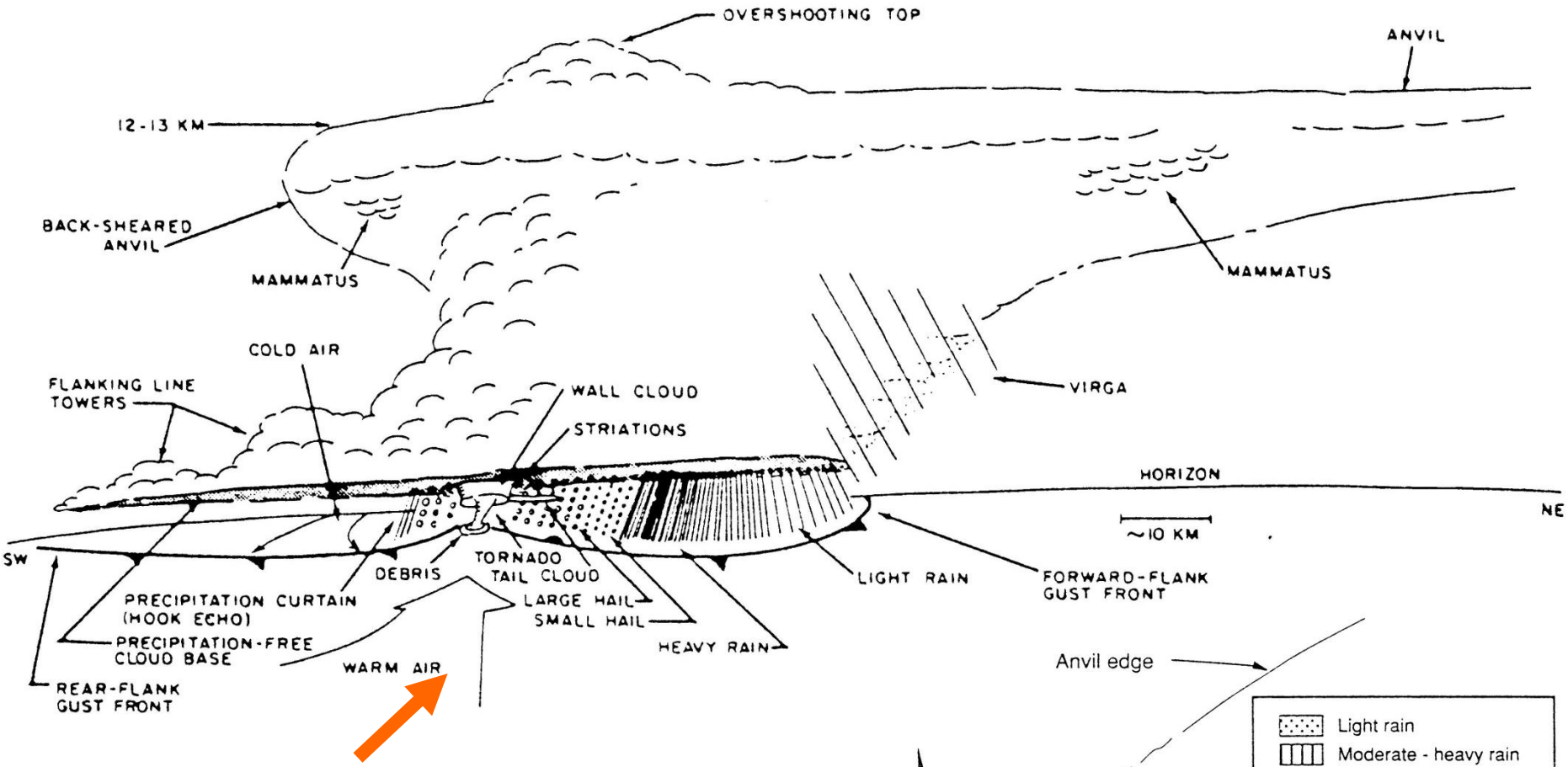

超級胞雷暴外觀試意圖

(Cloud features of supercell)

伴隨超級胞雲雨平面示意圖

(Precipitation features of supercell)

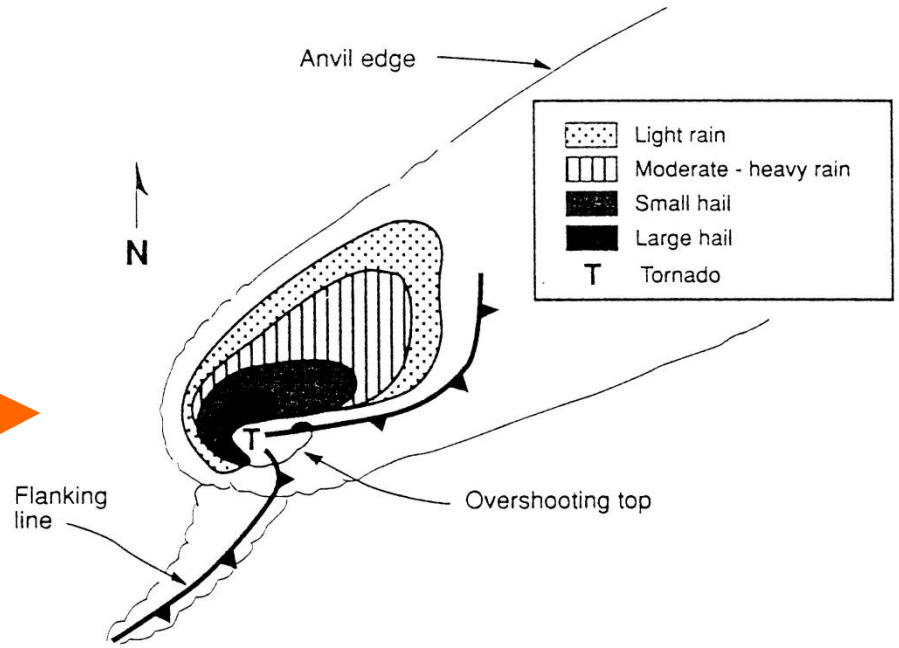

模擬超級胞之雲雨外觀 (Tufte 1997)

(3-D cloud feature of supercell)

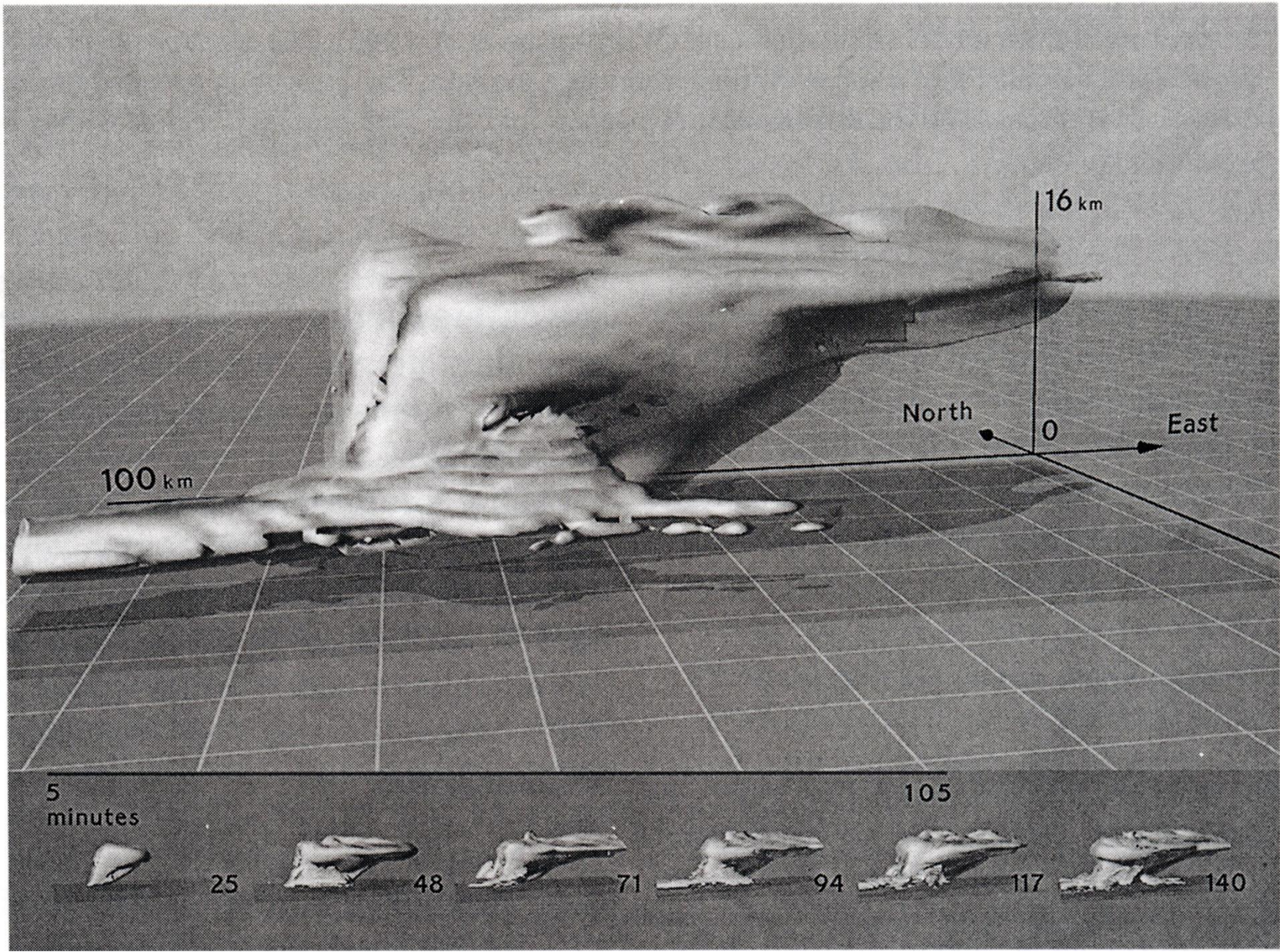

模擬超級胞之降水外觀及其水平剖面(Wilhelmson et al. 1990)

Cloud/precipitation of simulated supercell

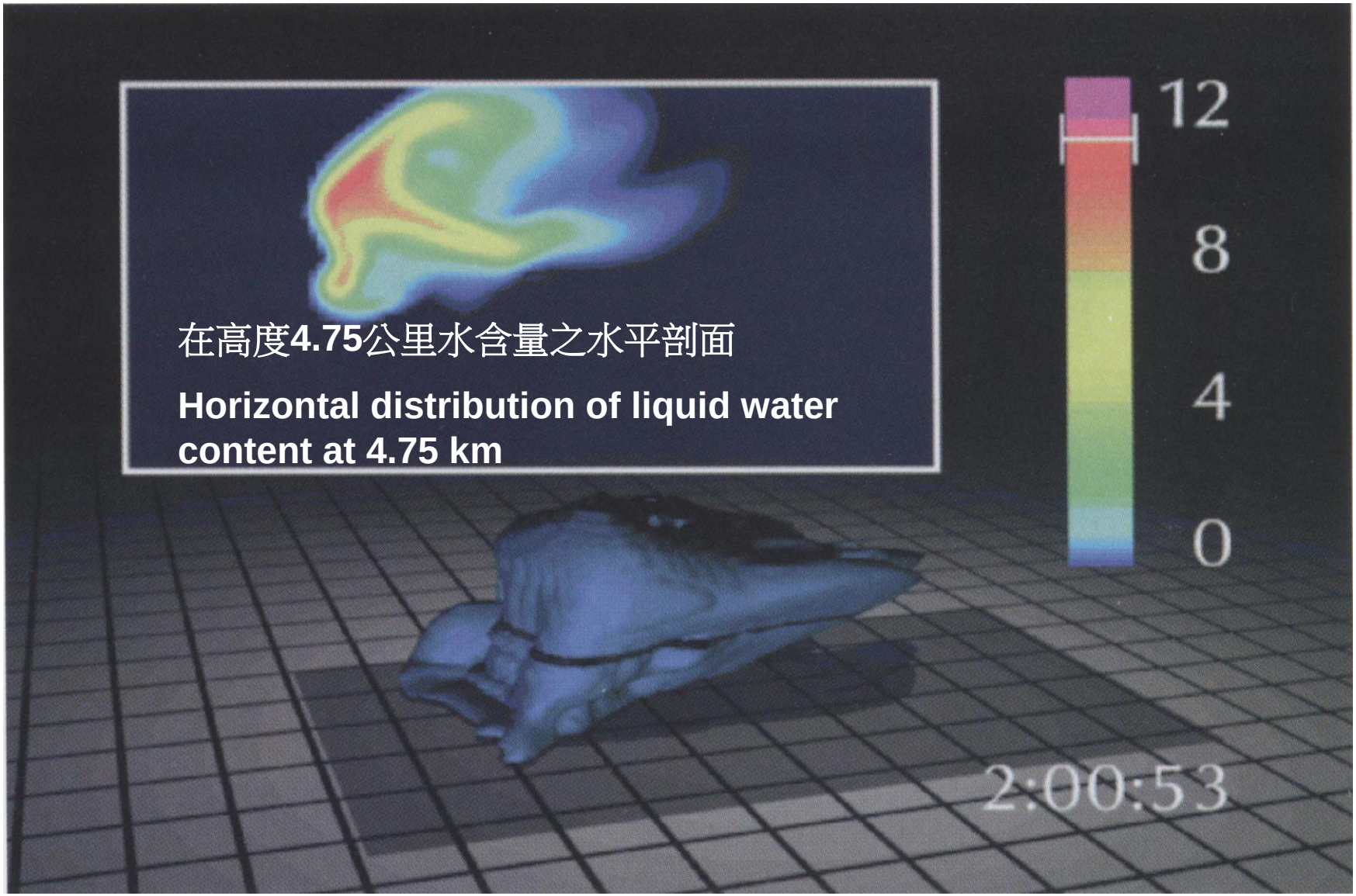

Rotating cloud associated with the mesocyclone of a supercell storm (Markowski and Richardson 2010)

Figure 8.17 A midlevel mesocyclone is the defining visual characteristic of a supercell storm. Little imagination is needed to sense the cyclonic vertical vorticity associated with the storm updraft. Photograph by Herb Stein (the Dopper On Wheels radar is in the foreground).

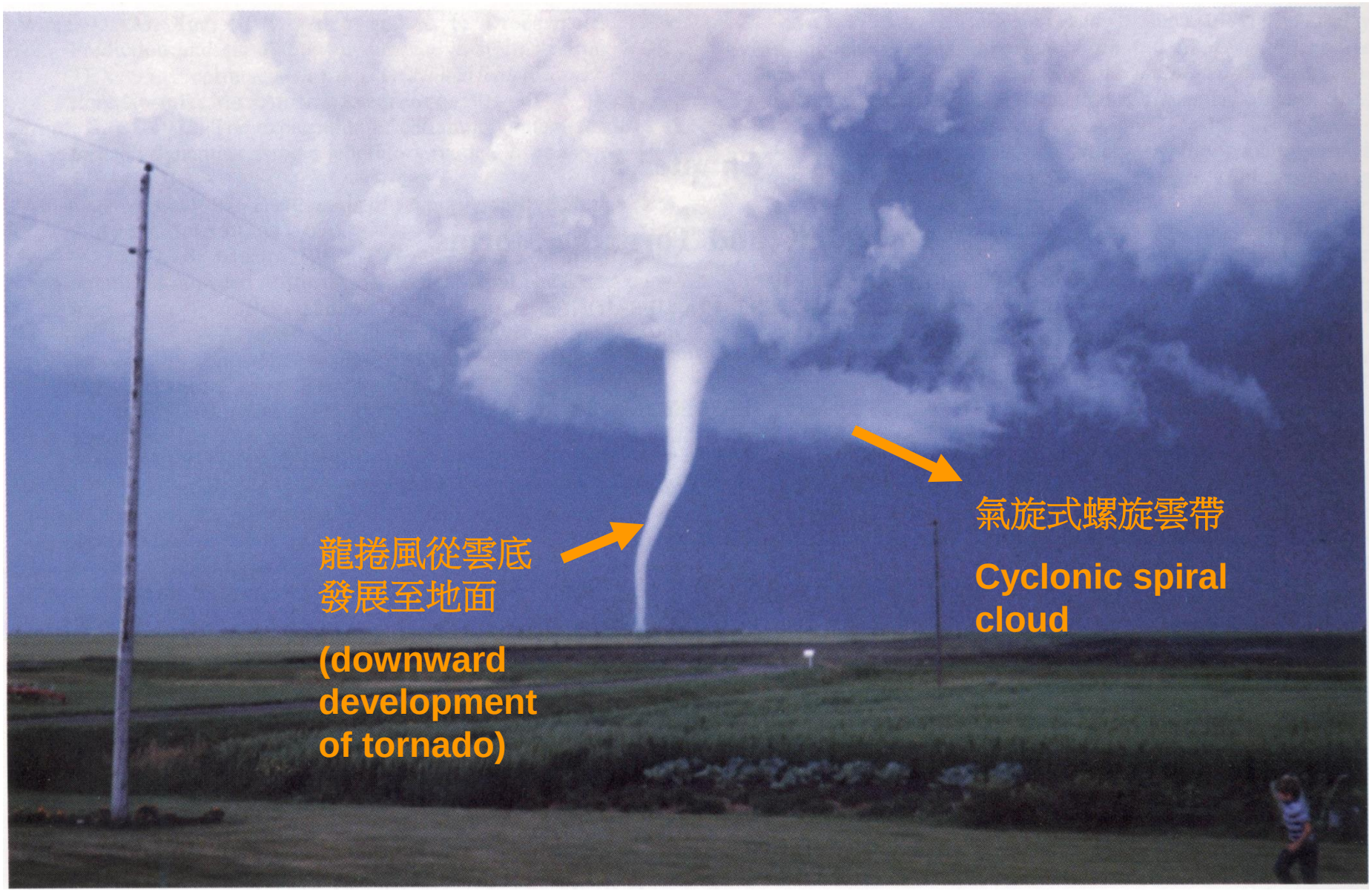
龍捲風從雲底
發展至地面
(downward
development
of tornado)
氣旋式螺旋雲帶
Cyclonic spiral
cloud

超級胞雷暴地面觀測特徵示意圖 (Lemon and Doswell 1979 and Davies-Jones 1986)

Surface feature of supercell

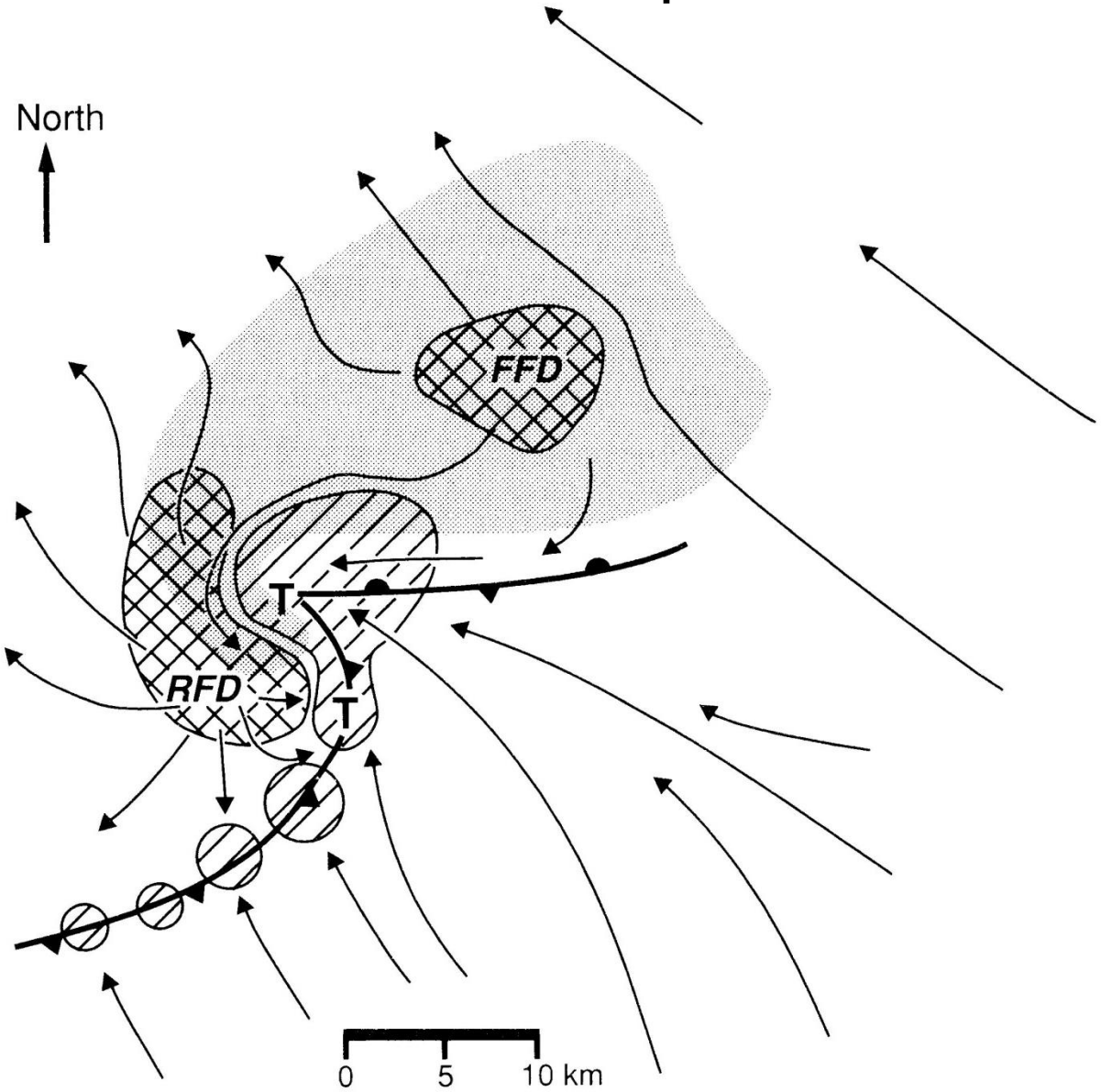

陰影區為雷達回波區

斜線為上升運動區位置

交叉斜線為下降運動區位置

T: 龍捲風可能發生位置

RFD (Rear-flank downdraft)

FFD (Forward-flank downdraft)

A real sample of radar PPI scan showing signatures of supercells (Markowski and Richardson 2010)

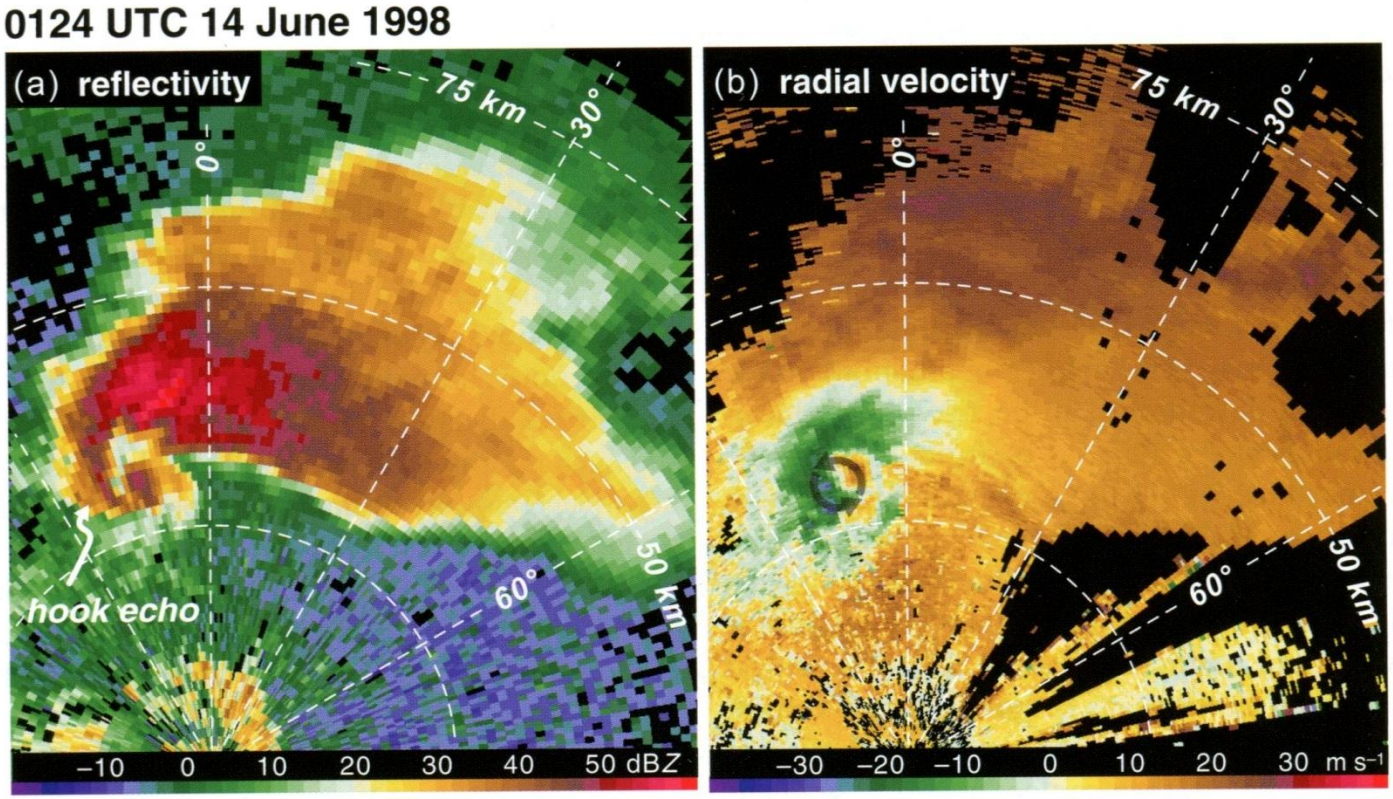

Figure 8.18 A hook echo in reflectivity data and an inbound–outbound couplet in radial velocity data are the defining radar characteristics of supercells in low-altitude radar scans. The images are (a) reflectivity and (b) radial velocity from the Oklahoma City, OK, radar at 0124 UTC 14 June 1998. The inbound–outbound radial velocity couplet is oriented such that the zero contour is approximately parallel to the radials, with inbound (outbound) velocities to the west (east), thereby implying cyclonic vertical vorticity.

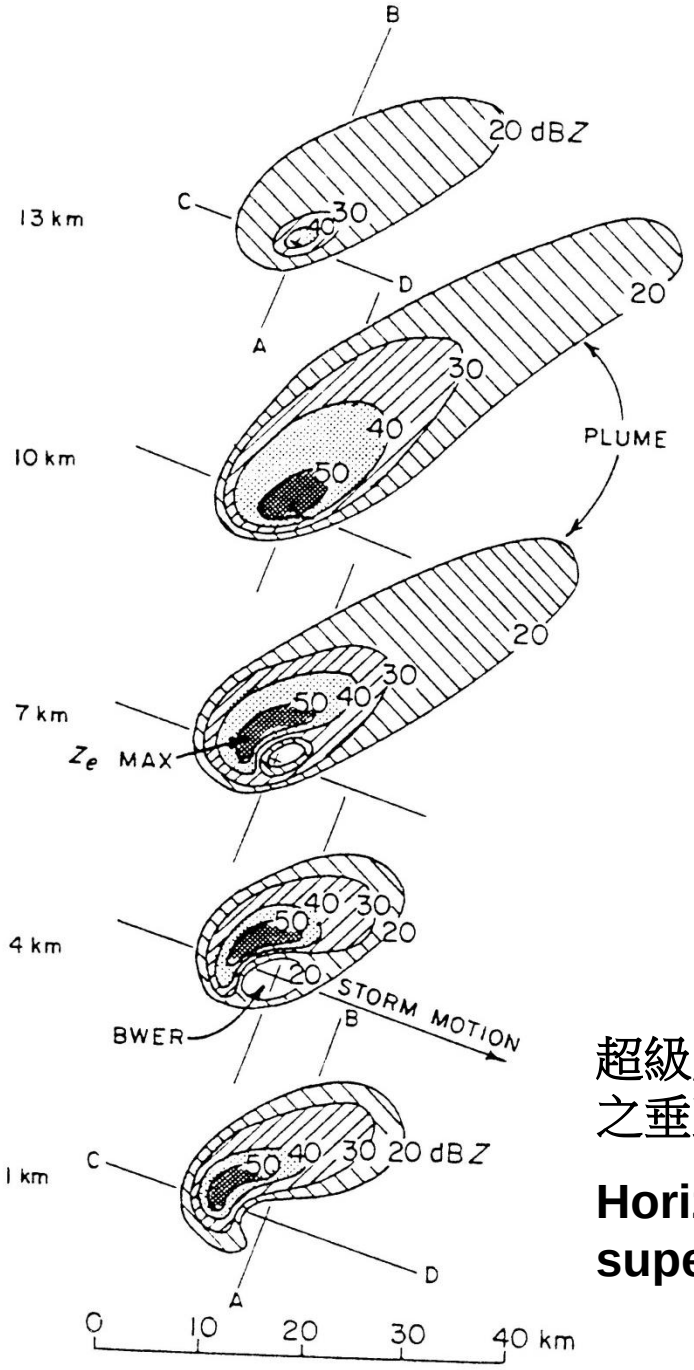

AB垂直剖面 (AB cross section)

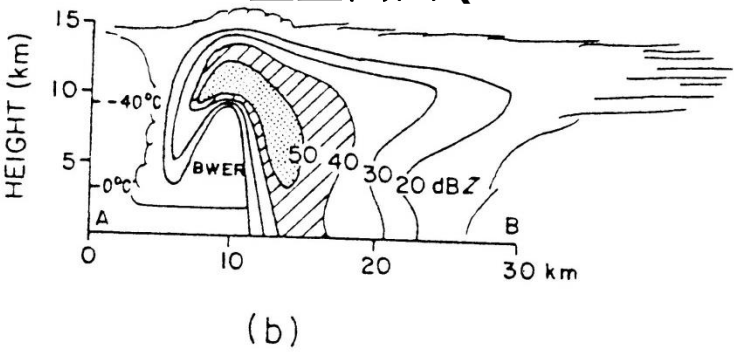

(b)

CD垂直剖面 (CD cross section)

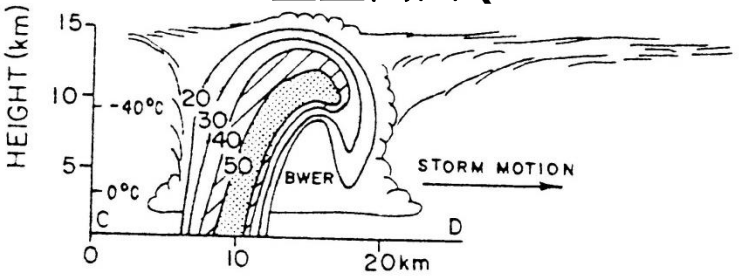

(c)

超級胞不同高度雷達回波結構與其在最強回波區之垂直剖面 **(Chisholm and Renick 1972)**

Horizontal structure of radar reflectivity of supercell at different heights

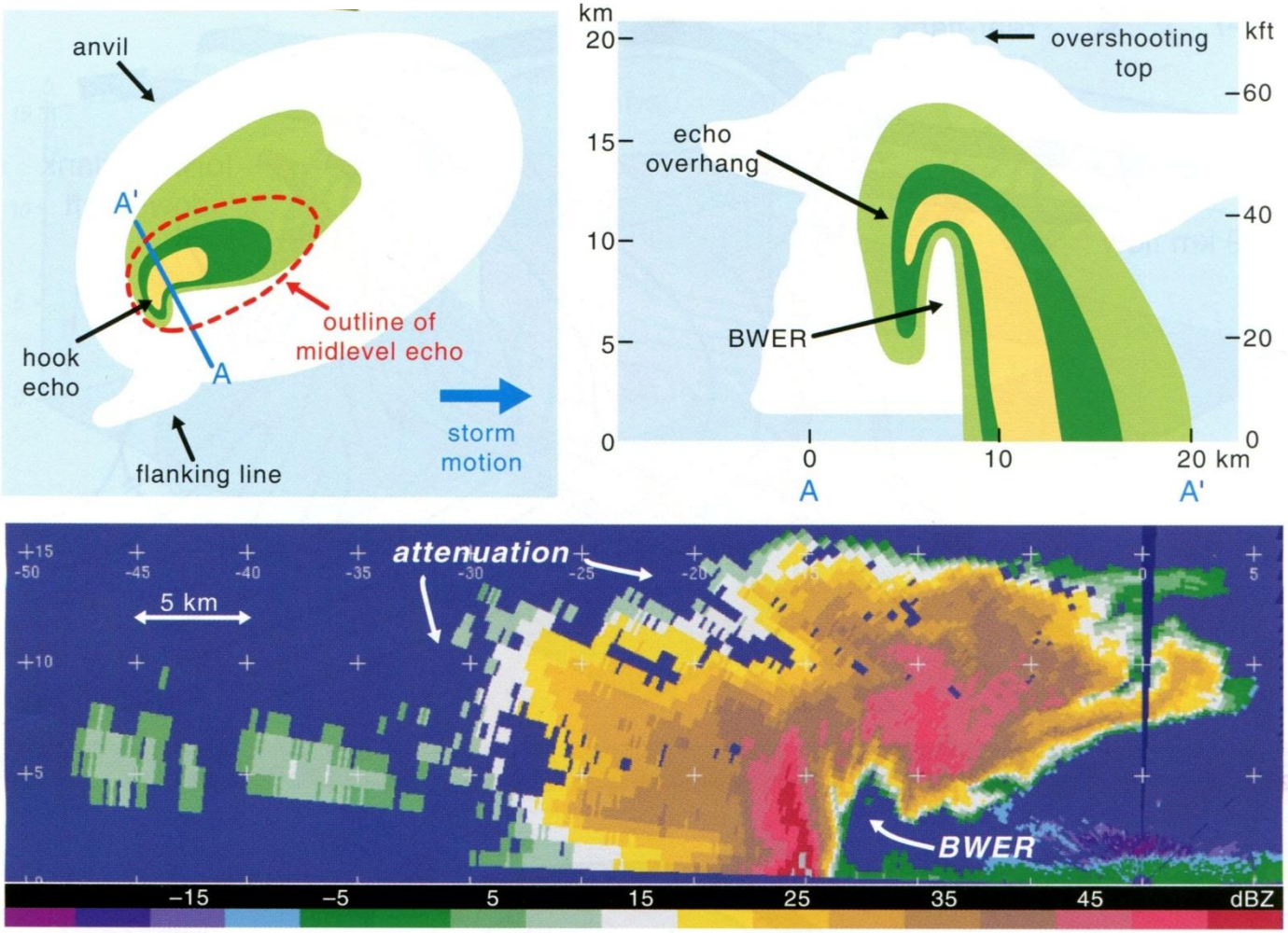

Figure 8.21 Top, schematic of the reflectivity structure of a supercell, showing the relationship between the bounded weak echo region (BWER), overshooting top, and hook echo. The green and yellow shading indicates weak, moderate, and high radar reflectivity visible at low levels (top left) and in a vertical cross-section (top right). Bottom, actual quasi-vertical cross-section of radar reflectivity factor in a supercell thunderstorm obtained from a helically scanning radar mounted in the tail of an aircraft at 2306 UTC 16 May 1995 during the Verification of the Origin of Rotation in Tornadoes Experiment (VORTEX).

WER (Weak Echo Regions)與BWER (Bounded Weak Echo Regions)
之雷達回波特徵示意圖

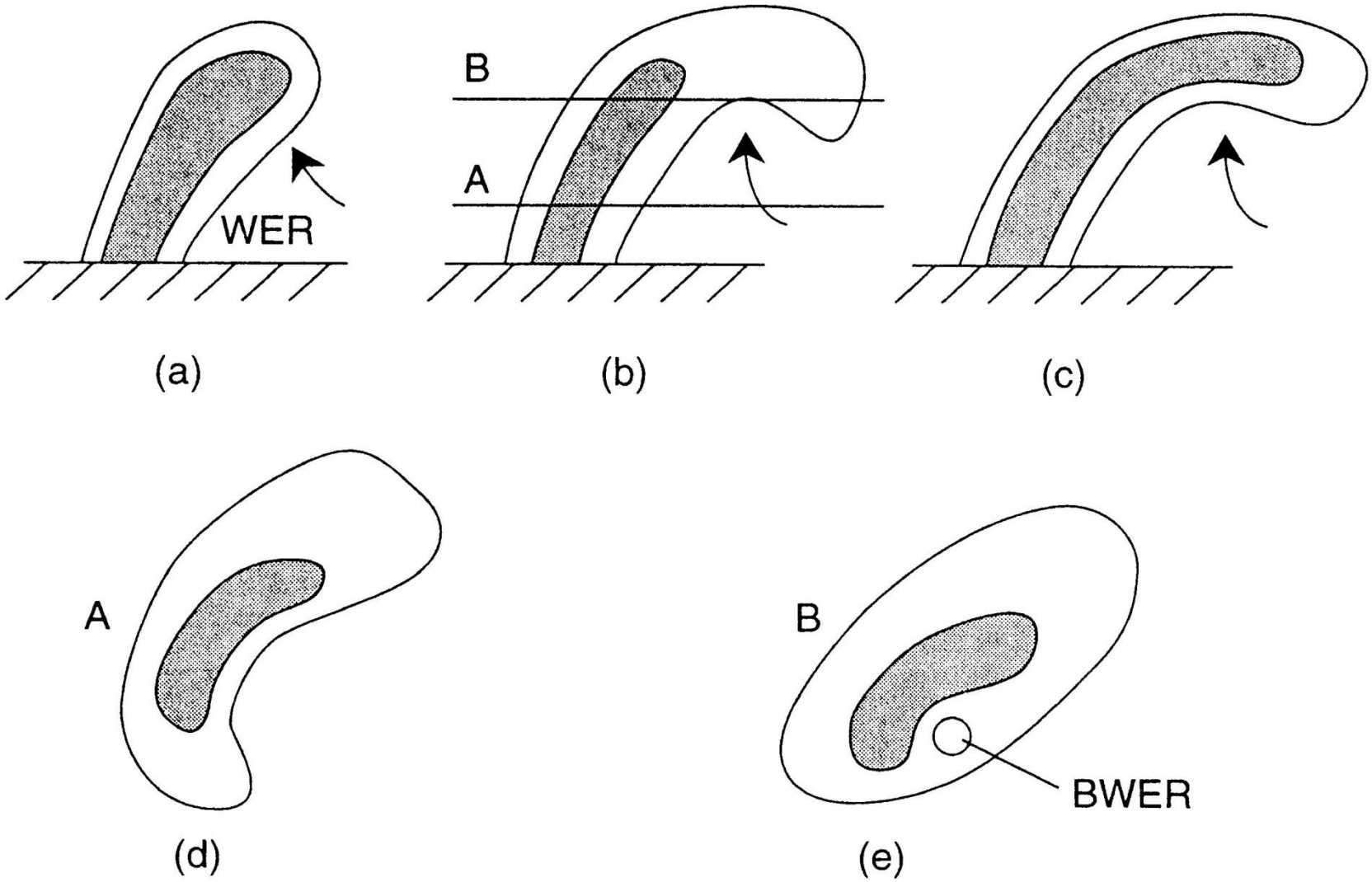

在不同的拖曳係數下, 冰雹直徑與其終端速度的關係

Terminal velocity of hail as a function of diameter

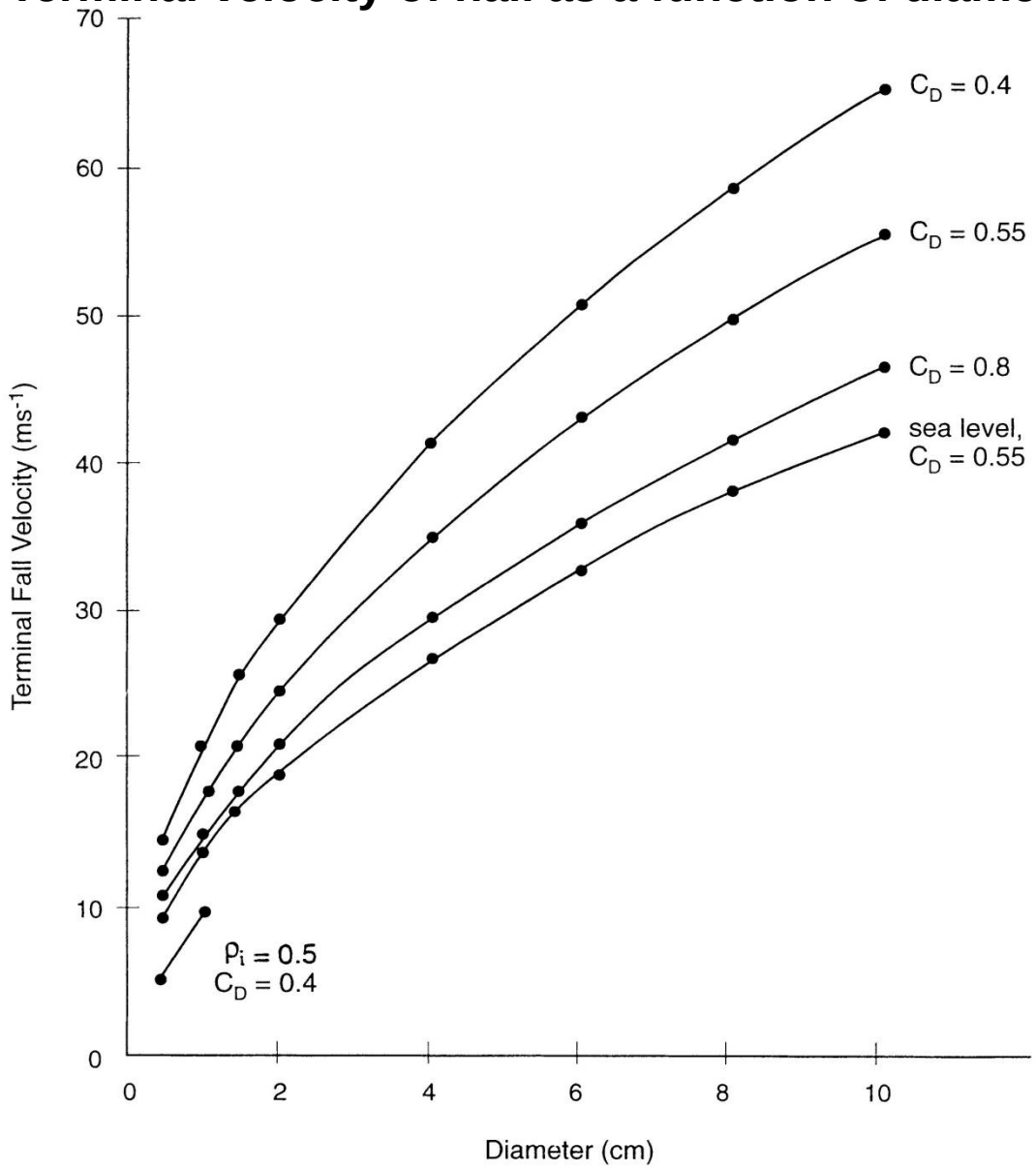

環境水平渦管與一對流胞交互作用所產生垂直渦度之示意圖 (Klemp 1987)

Vertical vorticity generated by the interaction between convective cell and environmental vertical shear

(伴隨中層旋轉氣流的擾動氣壓場與其氣壓梯度力的方向也顯示在圖中)

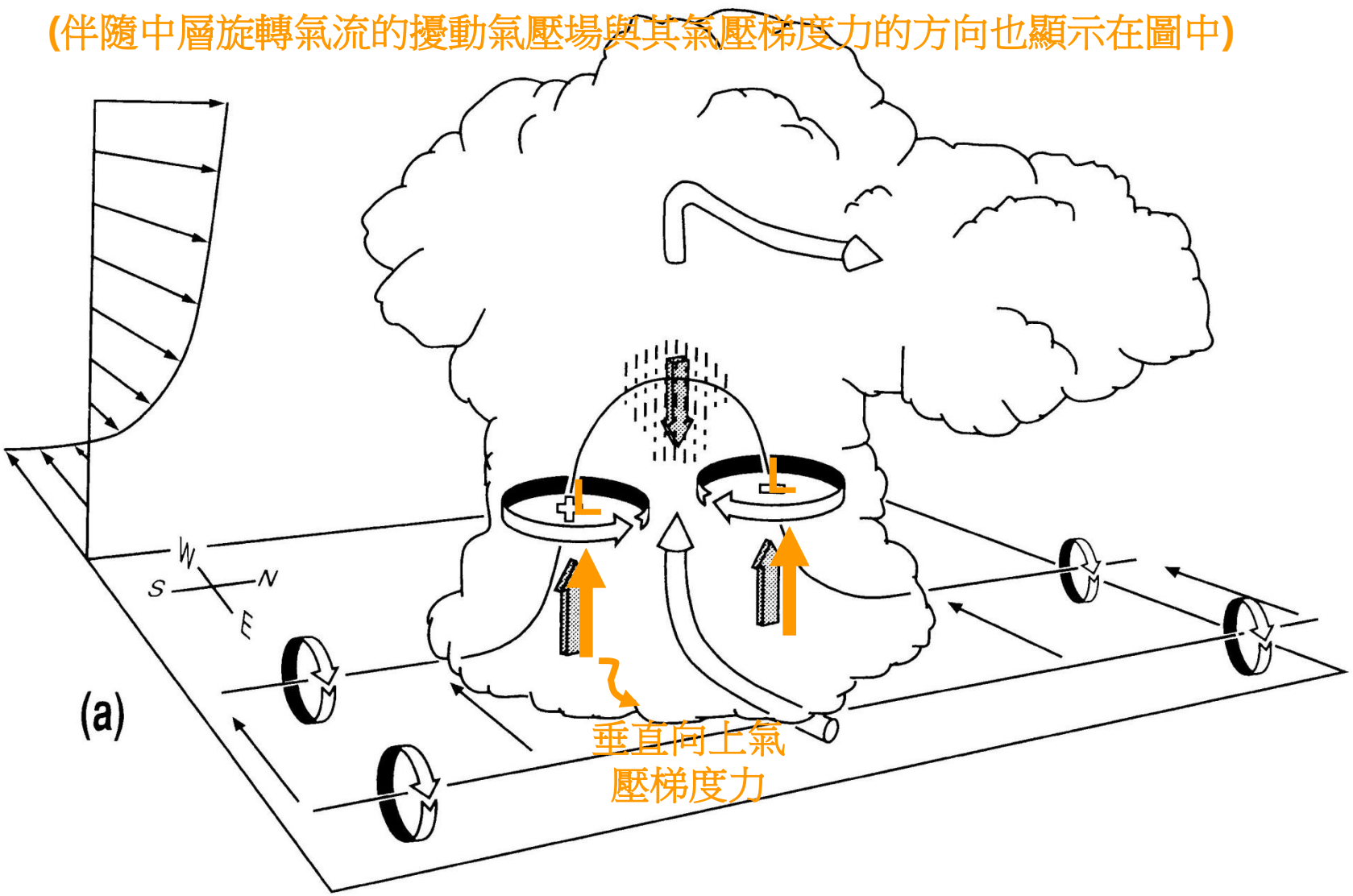

$$\nabla^2 p' \propto -2\rho_0 \frac{\partial v}{\partial x}\frac{\partial u}{\partial y} \propto \frac{1}{2}\zeta^2$$

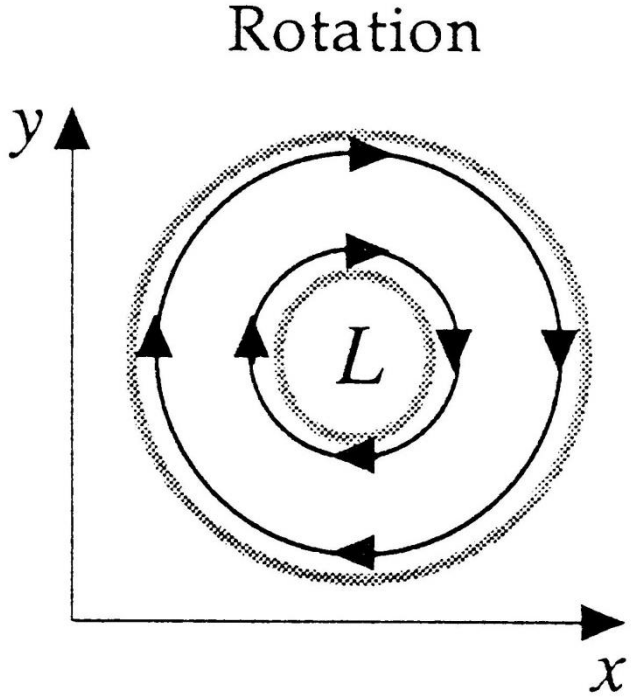

Houze (2014)

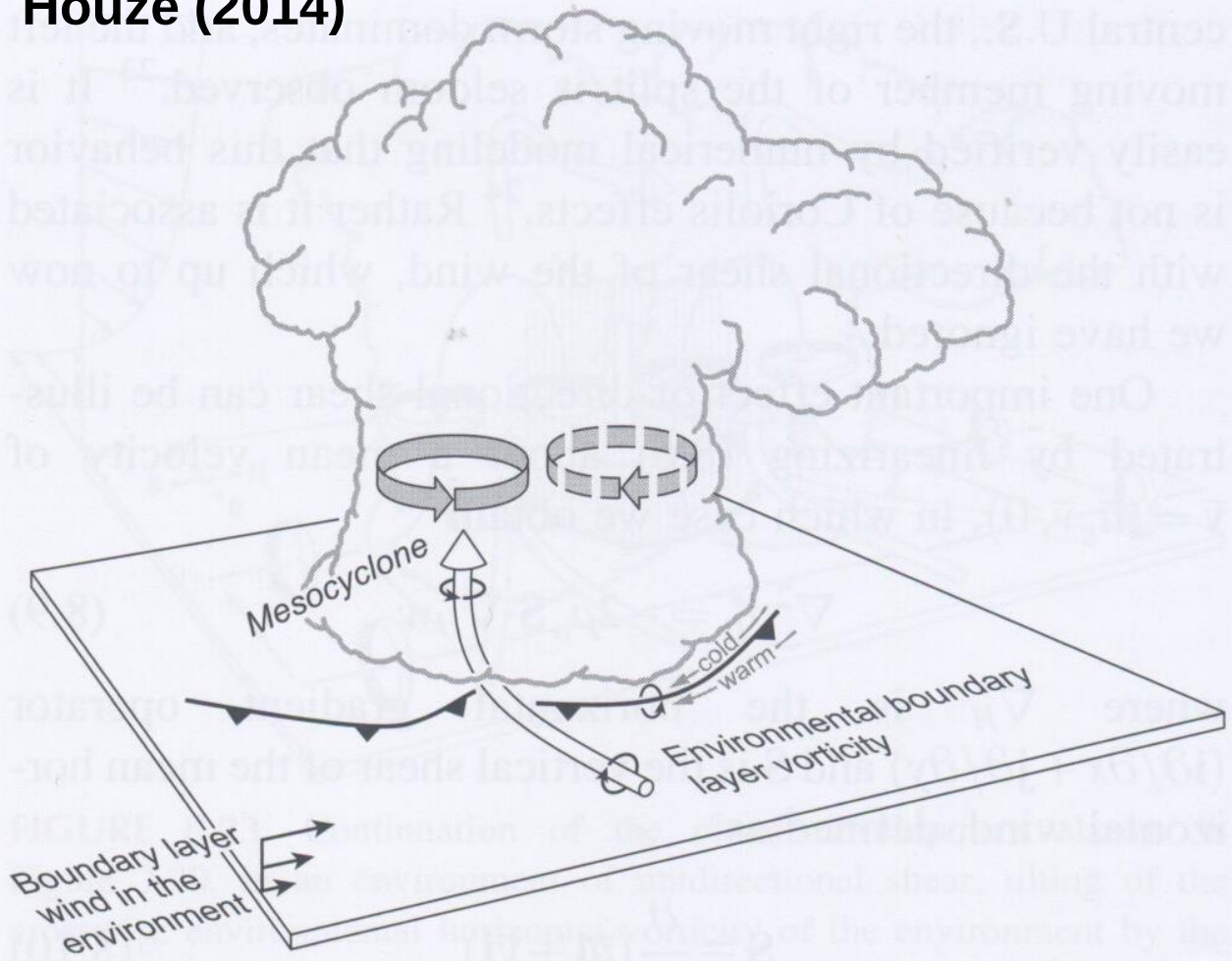

FIGURE 8.26 Schematic showing the vorticity of the air feeding into the updraft of a right moving supercell cumulonimbus in the Northern Hemisphere. The boundary-layer inflow has horizontal vorticity owing to shear of the wind in the boundary layer. Gust fronts are as in Figure 8.11a. The vorticity couplet aloft is due to tilting, as illustrated in Figures 8.23 and 8.24. The anticyclonic vortex is shown by a broken arrow to indicate weakening.

模擬超級胞之空氣塊軌跡 (Wilhelmson et al. 1990)

Trajectory of air parcel inside supercell

紅色線代表進入上衝氣流的空氣塊軌跡, 藍色線代表繞過上衝流而最後進入下衝流區的空氣塊軌跡

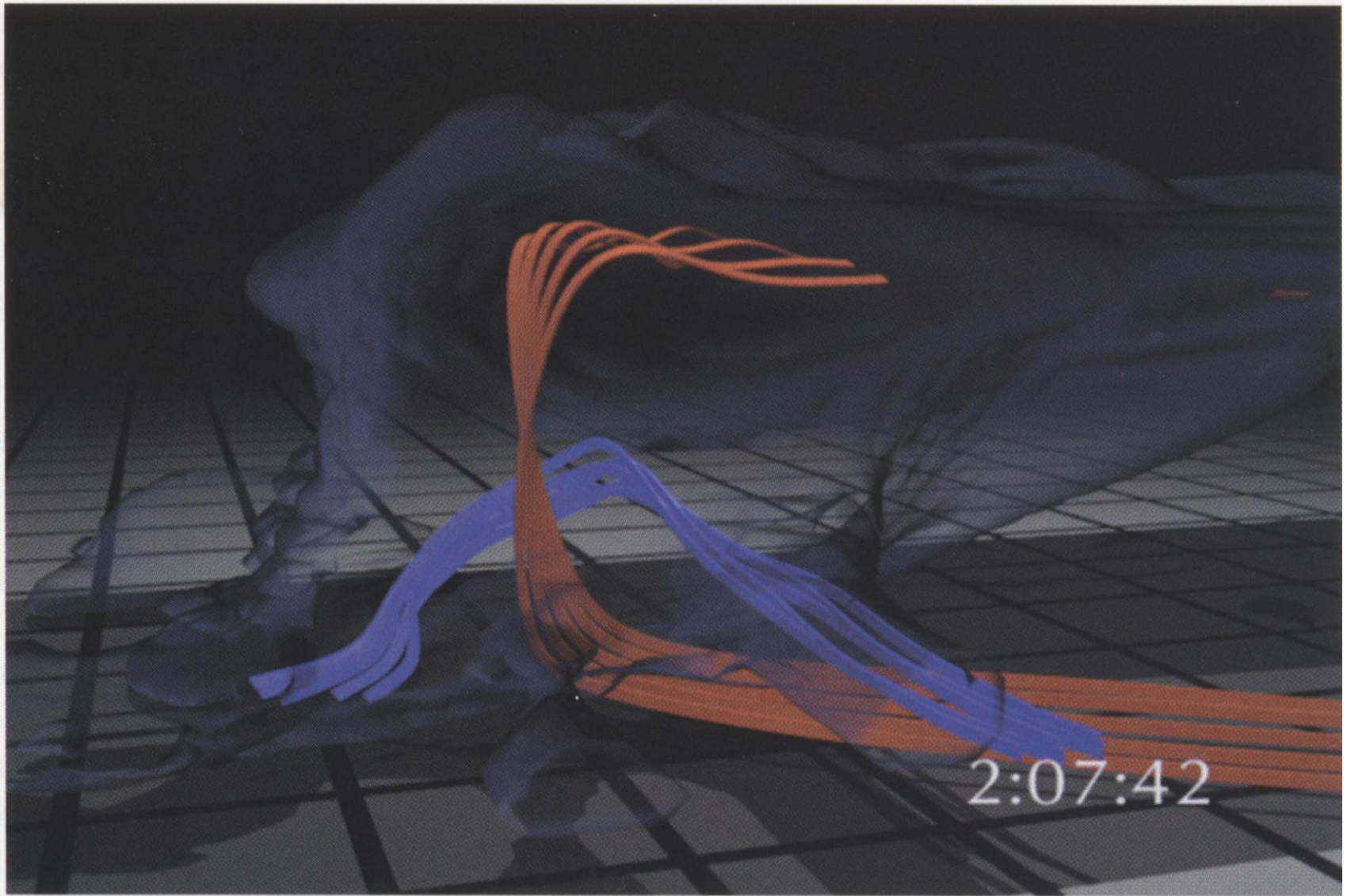

觀測與模擬之風暴發展與分裂 (Wilhelmson and Klemp 1981)

Storm splitting seen from observations and simulations

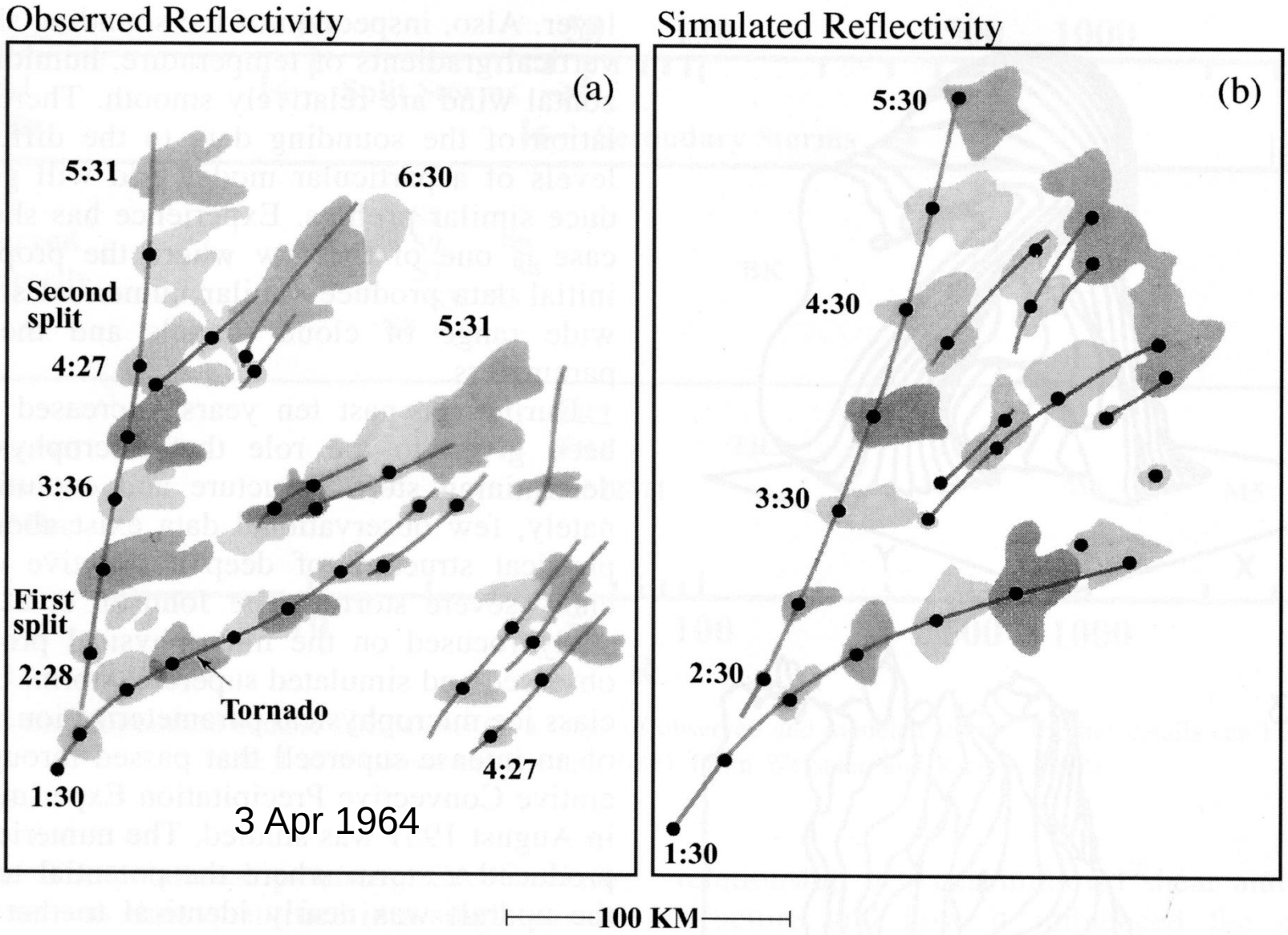

美國中部龍捲風暴之平均探空 **(Maddox 1976)**

Mean profile of winds associated with tornadic storms in the central US

風隨高度顯著順轉且風切向量隨高度順轉 **(directional shear)**

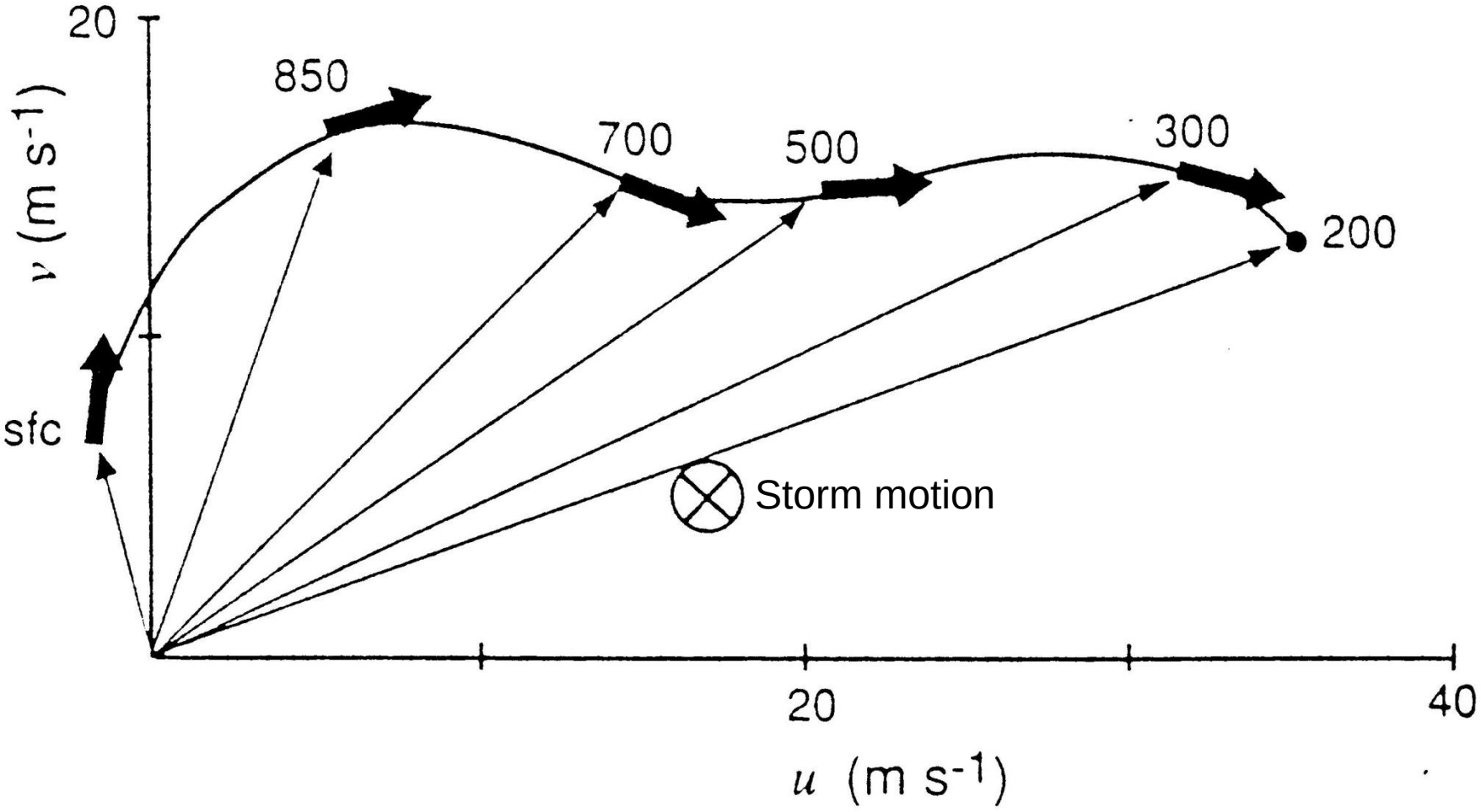

Directional shear favoring (disfavoring) the development of right (left) moving storms (Klemp 1987)

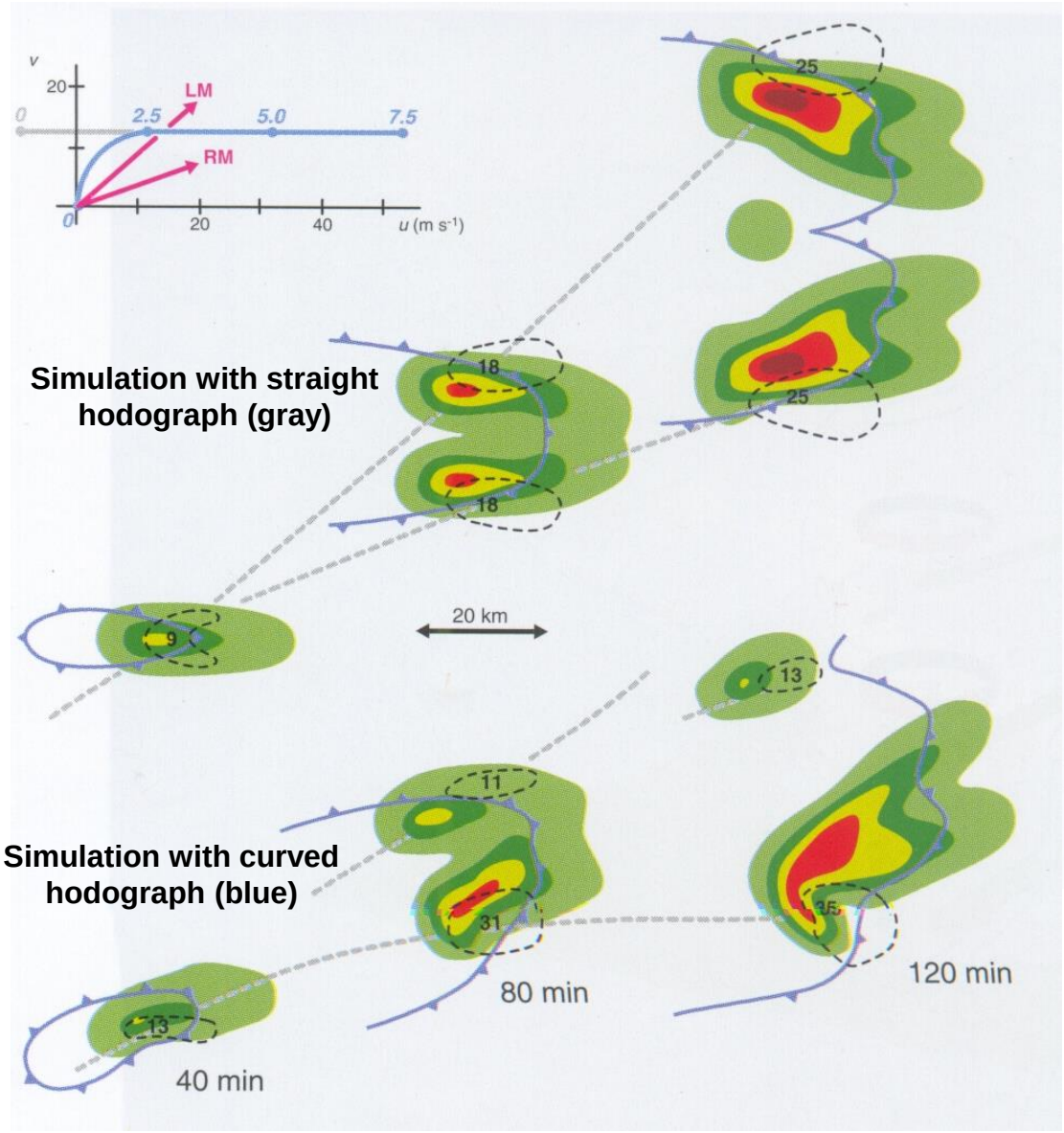

Figure 8.41 Plan views of cloud-model-produced, low-level rainwater fields for two simulations using, respectively, a straight hodograph (gray in lowest 2.5 km, blue above; numerals along the hodograph indicate altitude in km) and one with low-level clockwise hodograph curvature (blue). The straight hodograph produces storms with mirror-image symmetry, whereas the curved hodograph enhances the right-moving storm. The left- and right-moving storm motions are indicated on the hodographs with magenta arrows and are labeled 'LM' and 'RM', respectively. The dashed black contours enclose the regions of significant midlevel updraft, and the numerals indicate the location and magnitude of the maximum vertical velocity (m s^{-1}). Gust fronts are also shown. The gray dashed lines indicate storm motions. (Adapted from Klemp [1987].)

$$\nabla^2 p' \propto -2\rho_0 \left(\frac{\partial w}{\partial x}\frac{\partial u}{\partial z} + \frac{\partial w}{\partial y}\frac{\partial v}{\partial z} \right)$$

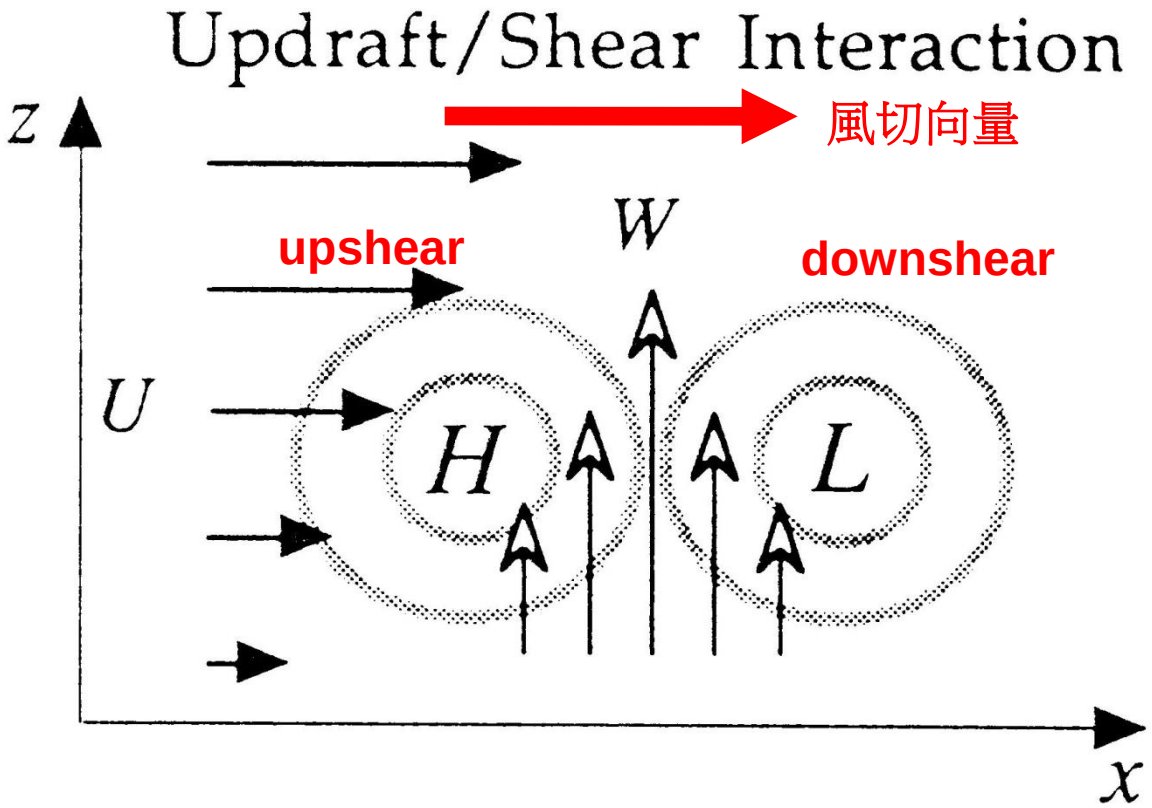

$$\frac{\partial w}{\partial x}\frac{\partial u}{\partial z}$$

風切向量

Shear vector

$$\vec{S} \equiv \frac{\partial u}{\partial z}\hat{i} + \frac{\partial v}{\partial z}\hat{j}$$

$$\frac{\partial w}{\partial x}\frac{\partial u}{\partial z} + \frac{\partial w}{\partial y}\frac{\partial v}{\partial z} = \vec{S} \cdot \nabla w$$

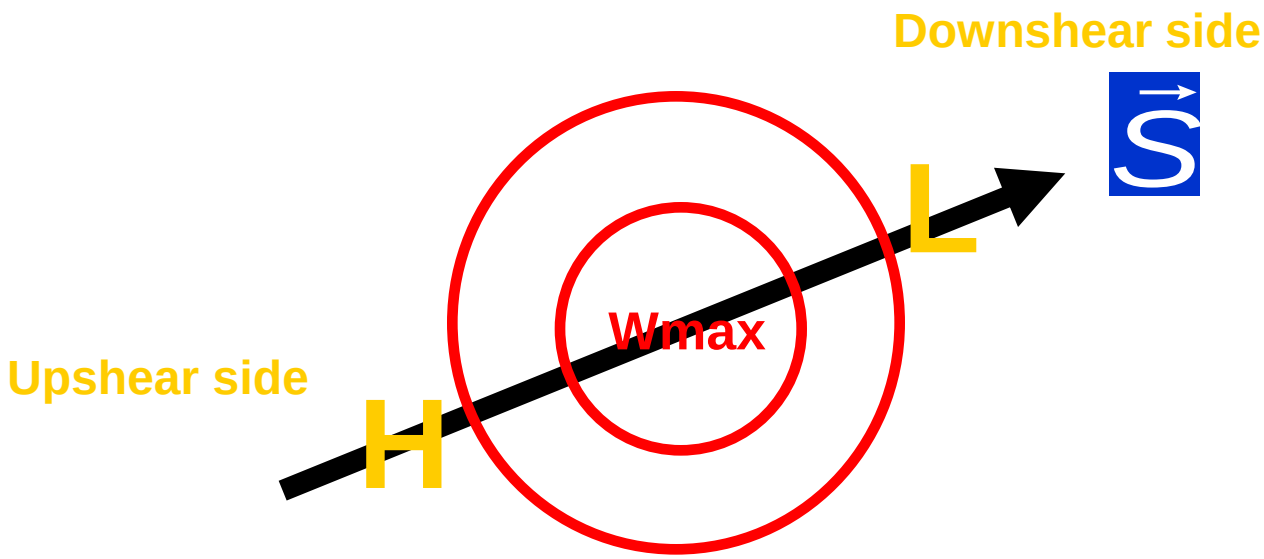

當環境風切向量不隨高度改變時, 超級胞雷暴與環境風切交互作用所產生的擾動氣壓分佈示意圖 (Klemp 1987)

Distribution of P' generated by the interaction between a convective cell and constant environmental vertical shear

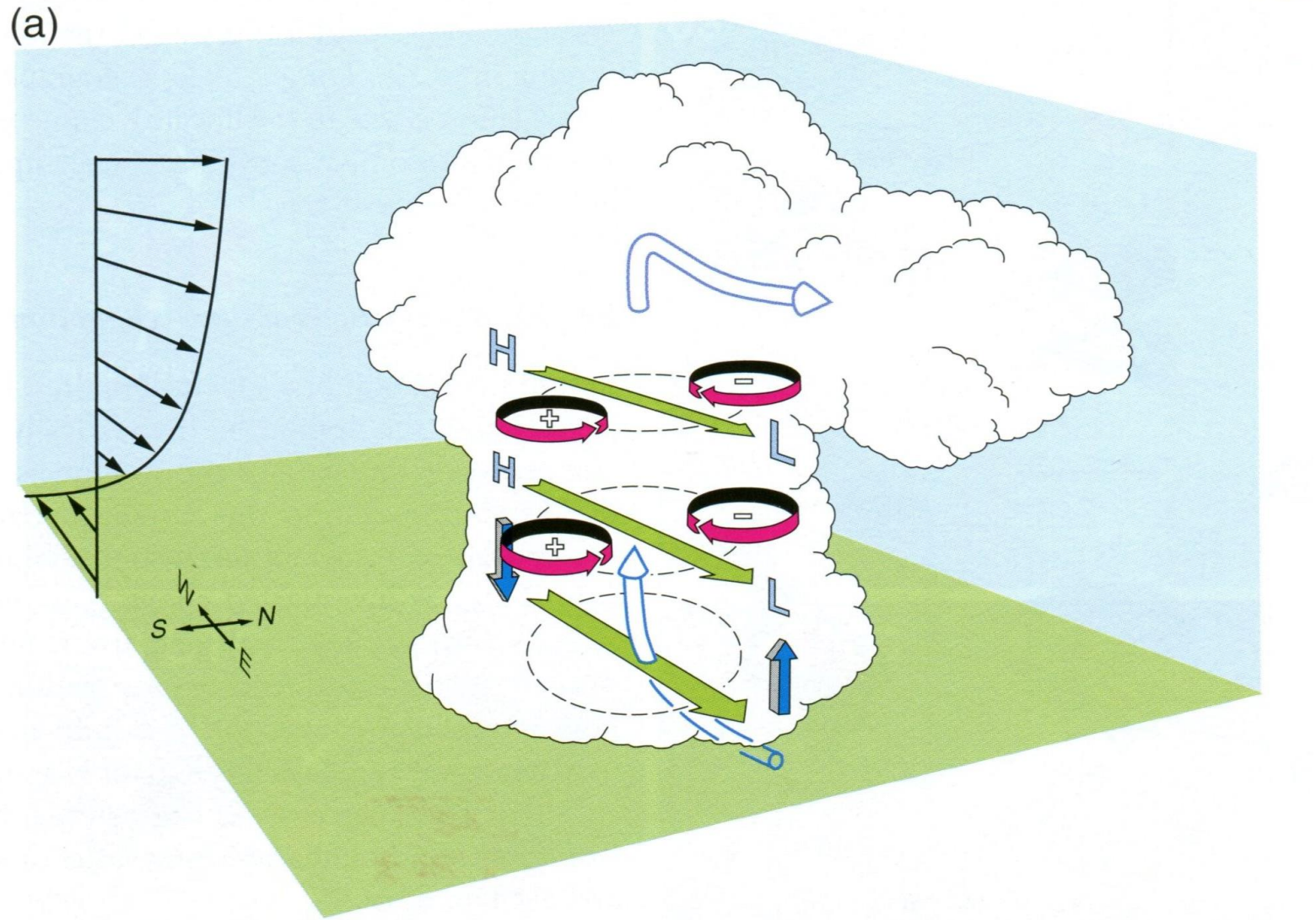

當環境風切向量隨高度順轉時, 超級胞雷暴與環境風切交互作用所產生的擾動氣壓分佈示意圖 (Klemp 1987)

Distribution of P' generated by the interaction between a convective cell and directional vertical shear

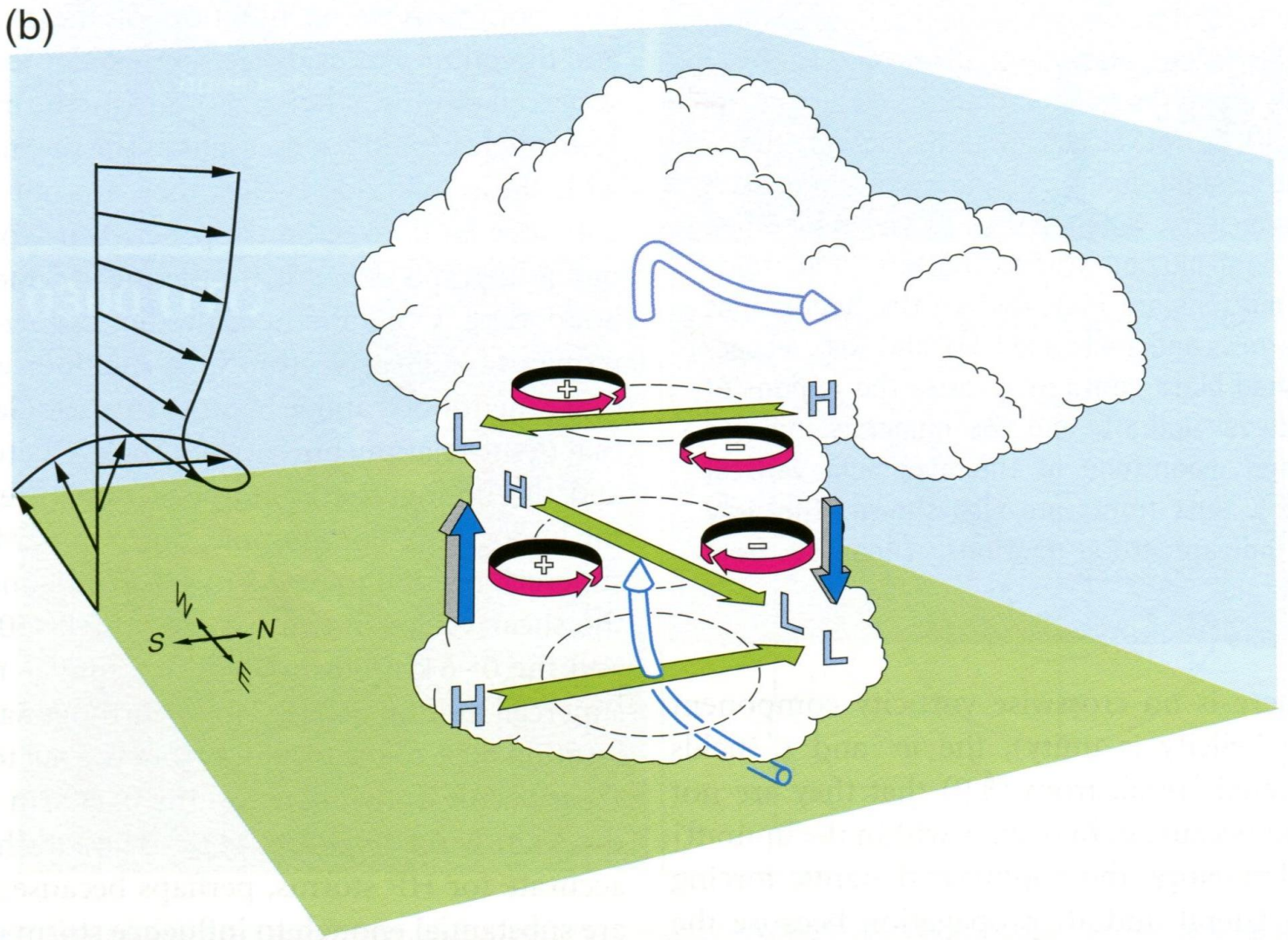

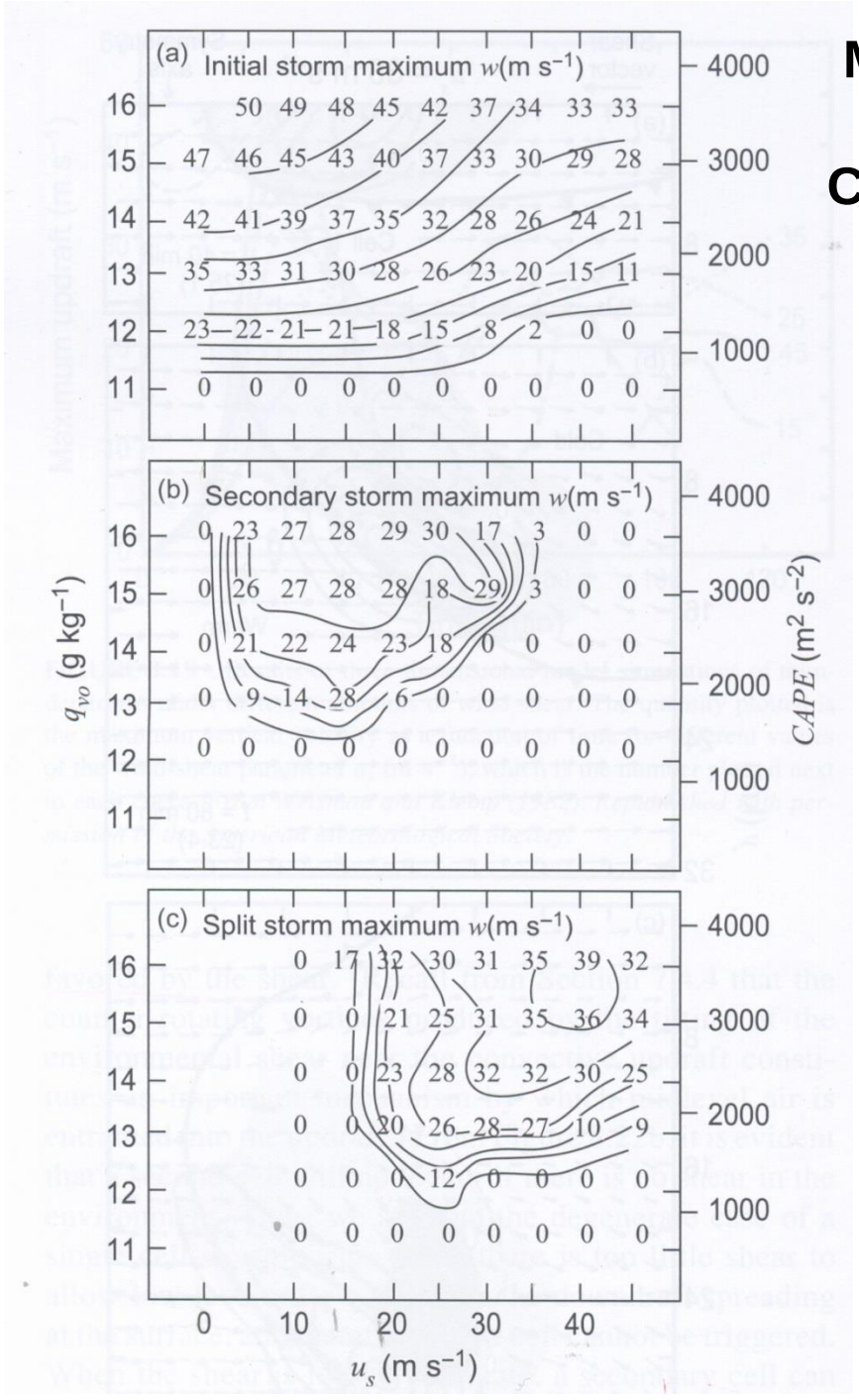

Maximum vertical velocity of model thunderstorms as a function of CAPE and wind-shear parameter (u_s) (Weisman and Klemp 1982)

(a) For initial storm, strength of updraft is proportional to CAPE, but inversely proportional to vertical shear

(b) For secondary storm, nearly zero shear or very strong shear is not favorable for the development of strong updrafts, regardless of CAPE; an optimal vertical shear appears to exist (RKW theory).

(c) For split storm, strongest updrafts exist in regions with large CAPE and vertical shear

These results imply that storm types (or updraft characteristics) may be classified by vertical shear and CAPE

$$CAPE \equiv \int_{LFC}^{EL} g\left[\frac{T_c - T_e}{T_e}\right]dz$$

LFC: Level of free convection

EL: Equilibrium level

Bulk Richardson number $R_{ib} = \dfrac{CAPE}{0.5(\Delta u^2 + \Delta v^2)}$

Δu

Δv

為6公里與500公尺高度平均風的差異量 (相當為垂直風切大小的量度)

Difference in mean winds between 500 m and 6 km (MSL)

觀測和模擬風暴種類與Bulk Richardson number的相關

Storm type as a function of Bulk Richardson number

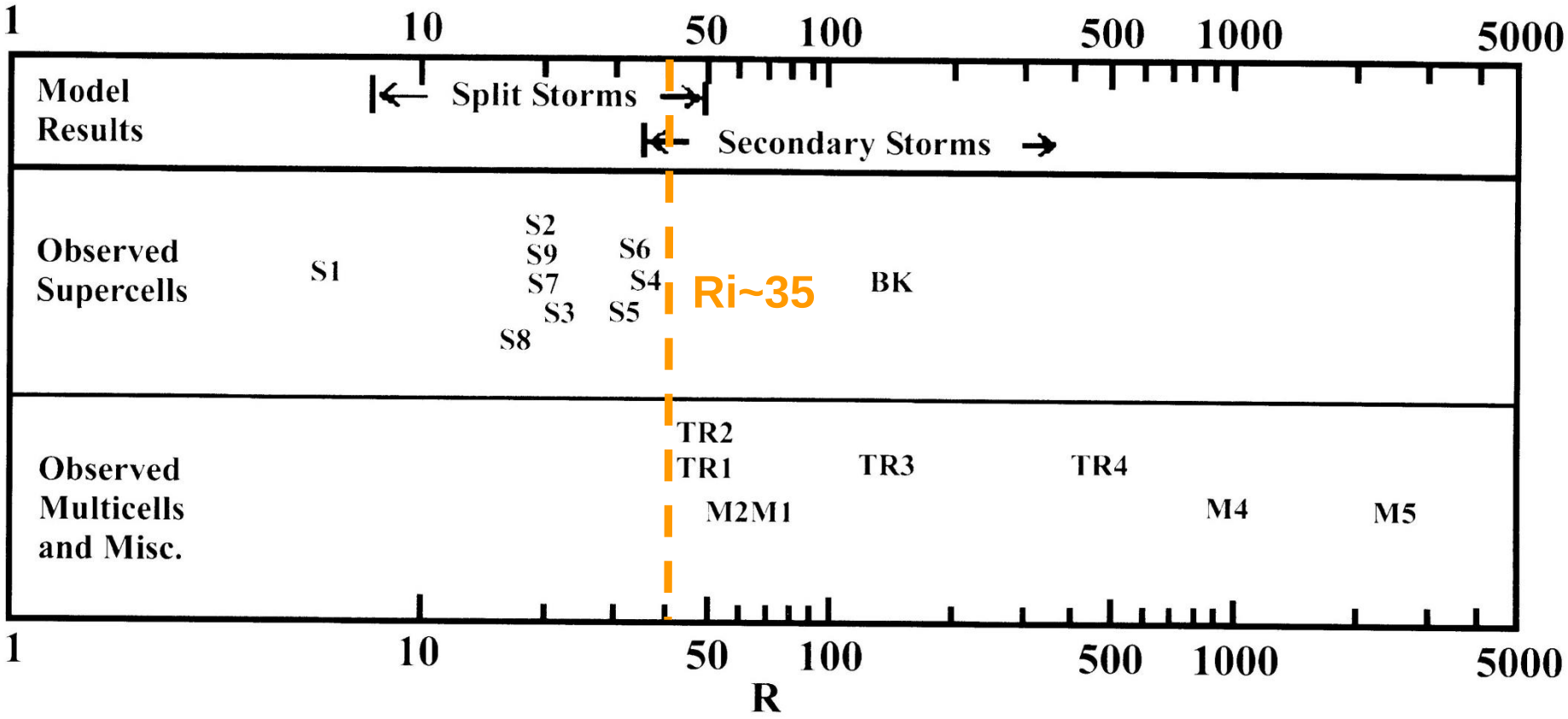

一般單胞風暴(Single Cell)與超級胞風暴(Supercell)之基本比較

Comparison between single cell and supercell

	單胞 (single cell)	超級胞 (supercell)
生命期(duration)	短(0.5-1 hour) short	長 long
上衝流的加速度來源(dw/dt)	浮力 (buoyancy)	氣壓梯度力 (PGF)
上衝流的旋轉特性 (rotation of w)	弱 (weak)	強 (strong)
上衝流的強度(w)	相對較弱(weaker)	強 (stronger)
上衝流的特徵 (character of w)	較不steady (unsteady)	quasi-steady
發展的環境 (environment)	弱風切 (weak shear)	強風切 (strong shear)
伴隨天氣 (weather)	較不劇烈 (less severe)	劇烈 (severe)
發生的緯度 (location)	低緯或中緯度 (low or mid lat.)	主要在中緯度 (mid lat.)

由超級胞所組成的線狀對流系統示意圖(Lilly 1979)

Line convection composed by supercells

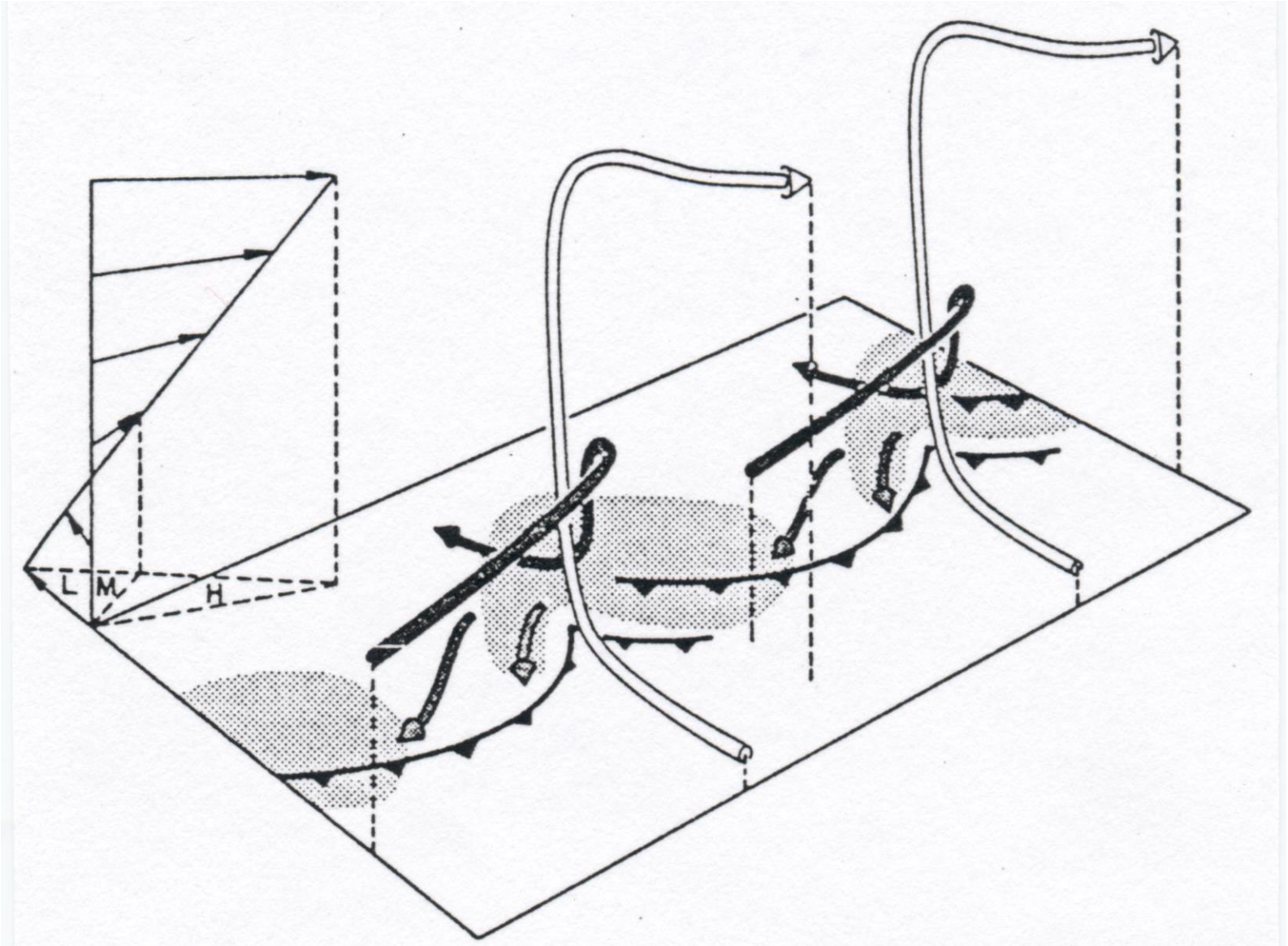

美國奧克拉荷馬州東部所觀測到的超級胞對流線

(在飛機上所拍攝的照片, by P. Sinclair, 26 May 1973)

Photo showing a supercell-composed convective line

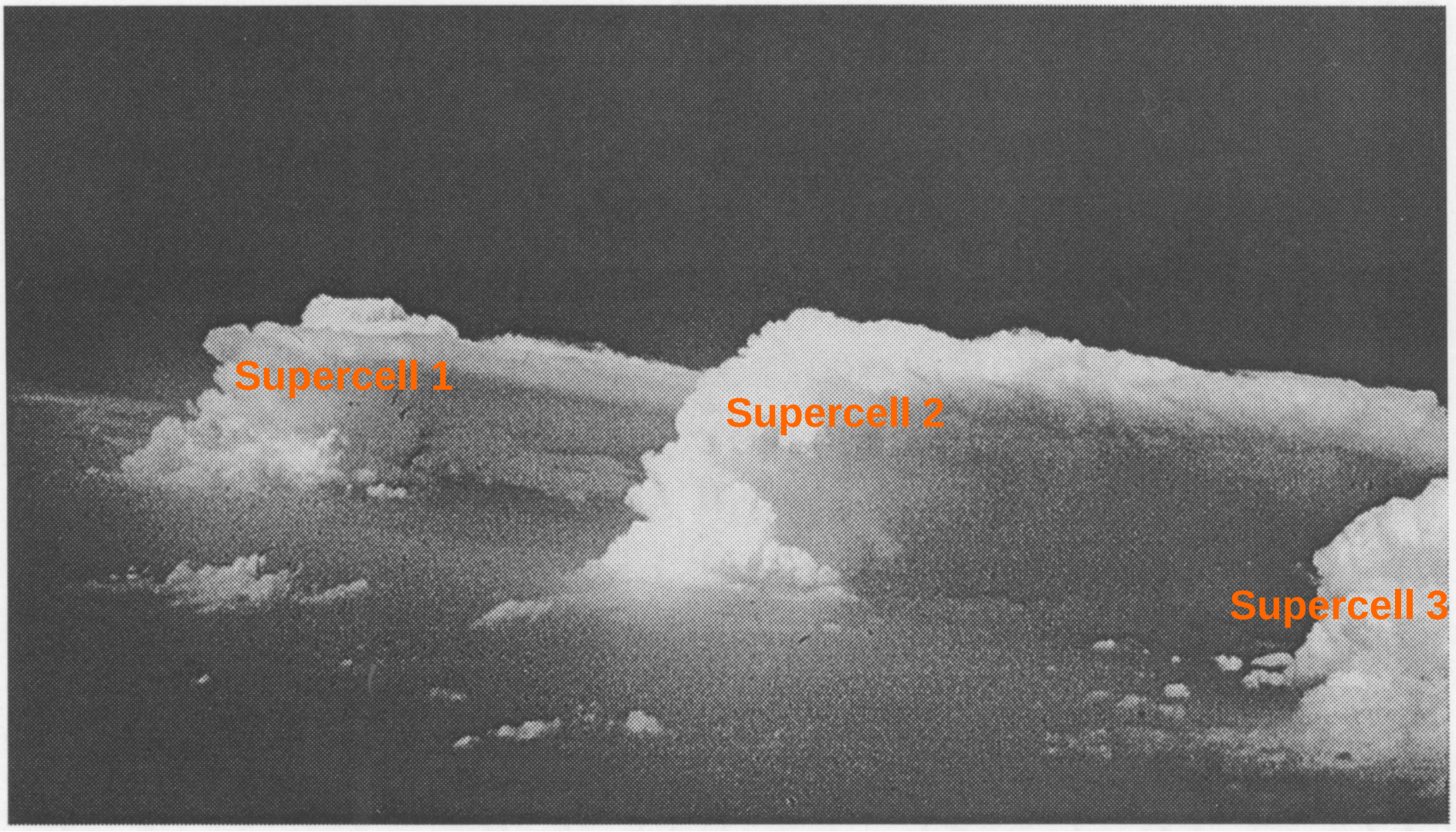

美國奧克拉荷馬州劇烈颱線之環境平均風徑圖**(Bluestein and Jain 1985)**

Environmental hodograph associated with severe squall lines in Oklahoma

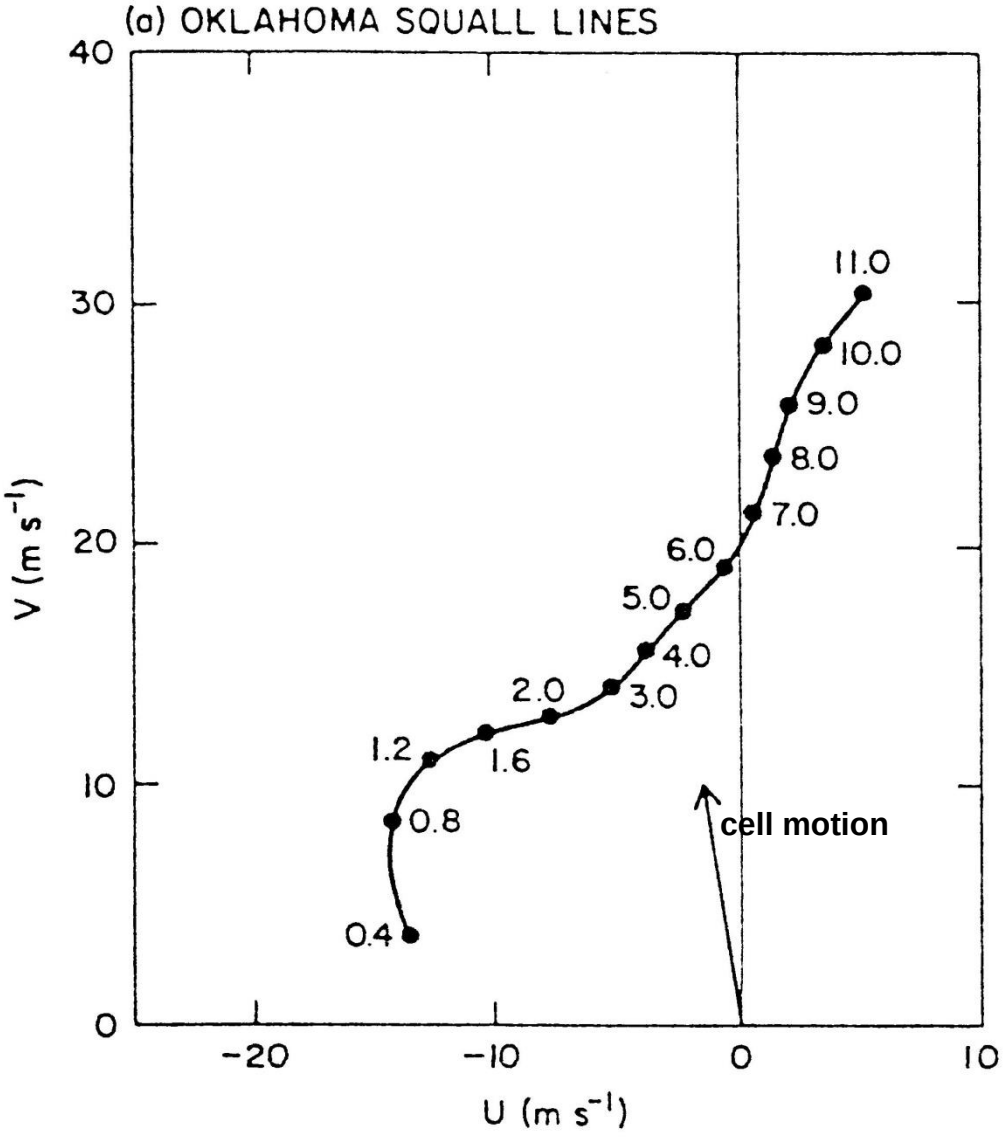

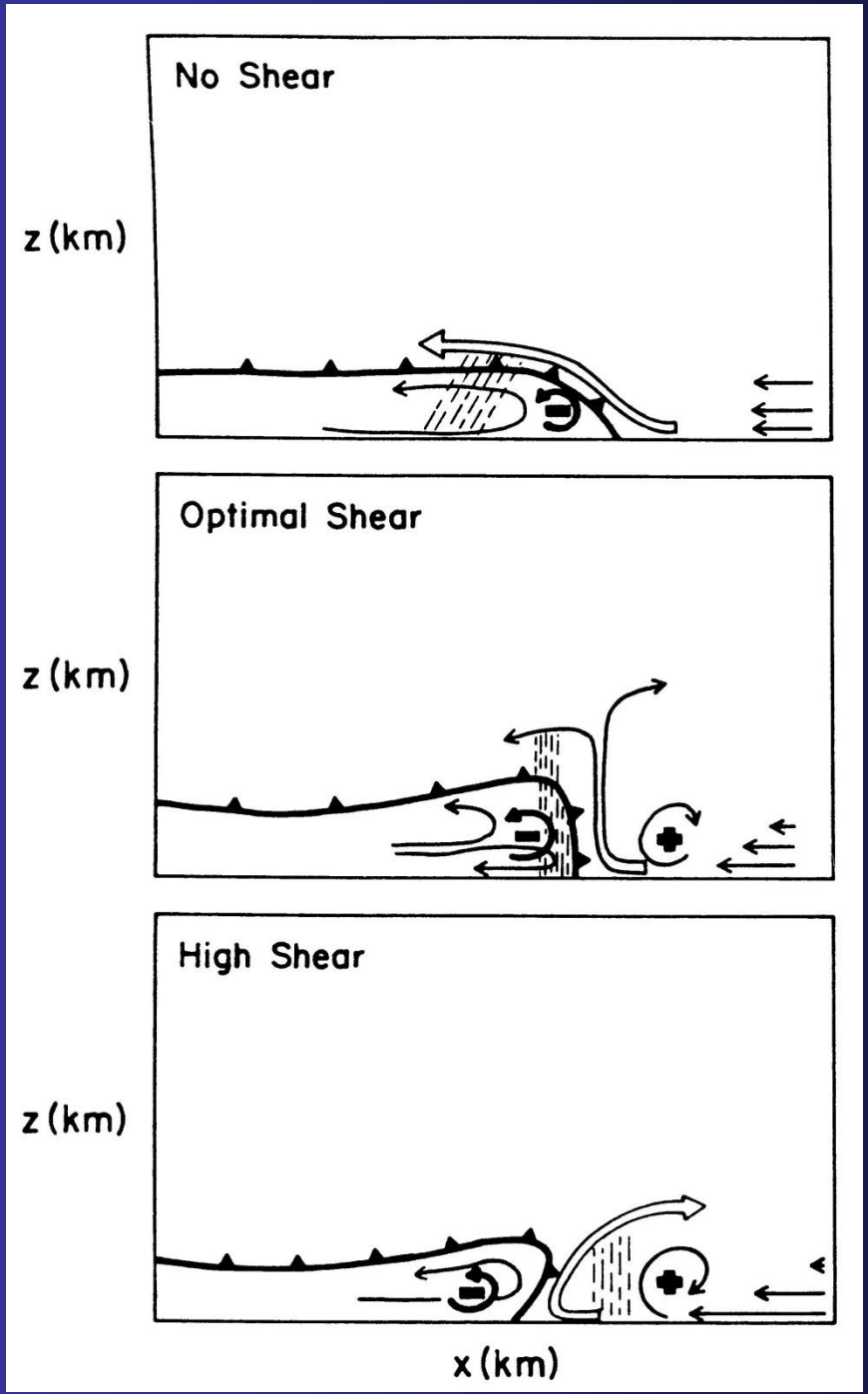

鋒面前緣上衝流特性與環境垂直風切的相關 **(Parsons 1992)**

Strength of frontal updrafts at different environmental vertical shear

正負號分別代表伴隨環境垂直風切與鋒後冷池的水平渦度

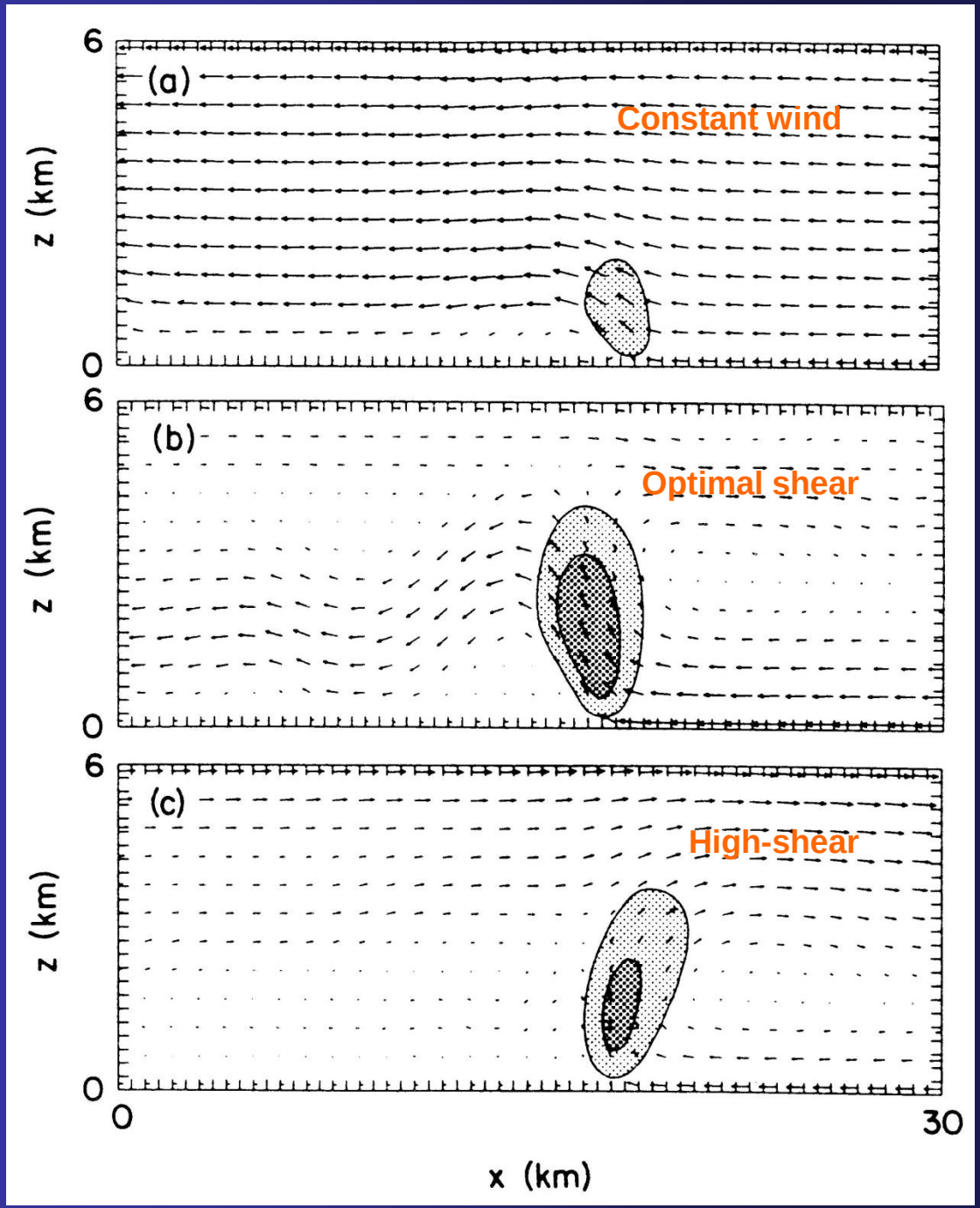

在不同的環境垂直風切下所模擬出的鋒面上衝流的特徵
(Parsons 1992)

Frontal updrafts simulated with different environmental vertical shear

淺陰影代表垂直速度大於2.5 m/s

深陰影代表垂直速度大於5 m/s

Light shading (w > 2.5 m/s)

Dark shading (w > 5 m/s)

鋒面前緣上衝流大小與垂直風切的相關 (Parsons 1992)

Strength of frontal updrafts as a function of ambient vertical shear